



UNIVERSITÀ DEGLI STUDI DI MILANO
FACOLTÀ DI SCIENZE DEL FARMACO
Department of Pharmaceutical Sciences
PhD Course in Pharmaceutical Sciences
XXIX Cycle

**DESIGN AND DEVELOPMENT OF CAPSULAR MOLDED
DEVICES FOR MODIFIED RELEASE OF DRUGS**

Tutor: **Dr. Lucia Zema**

Coordinator: **Prof. Marco De Amici**

FEDERICA CASATI

R10451

Academic year 2015/2016

*“À Maurice et Florie:
c’est parfait.”*

“The roots of education are bitter, but the fruit is sweet.” Aristotle

Acknowledgments

I would like to acknowledge:

Professor Andrea Gazzaniga for giving me this great opportunity; Dr. Lucia Zema for accepting to be the supervisor of my PhD, for encouraging me in my work. Your advice and criticism taught me how to improve.

Please accept the assurances of my highest consideration and respect.

Dr. Francesco Briatico Vangosa, for accepting to be the advisor of my PhD thesis and, together with Dr. Francesco Baldi, for broadening my horizons to different fields of knowledge.

Allow me to express my deepest thanks.

Professor Jürgen Siepmann, for giving me the excellent opportunity to work in your laboratory and also for accepting to be the advisor of my PhD thesis. Professor Florence Siepmann, Dr. Youness Karrout and Dr. Christel Neut for having welcomed me, for your continuous availability and for everything you've taught me.

I'm really grateful, please accept my heartfelt thanks.

Table of contents

❖ Preface.....	pag. 1
Annex.....	pag. 9
❖ Chapter I.....	pag. 11
❖ Chapter II.....	pag. 45
❖ Chapter III.....	pag. 72
❖ Conclusions.....	pag. 107

Preface

Polymers have a widespread impact on modern society, especially plastics, which represent the most diffused polymeric components of all the objects used in everyday life.

Plastics, from latin *plasticus* (“of molding”) or ancient Greek πλαστικός (*plastikós*) and πλάσσειν (*plássein*, “to mold, form”), have indeed the ability to be molded, shaped, cast, extruded, drawn, thermoformed, or laminated into a final product such as plastic parts, films, and filaments. After the plastic revolution of late 19th and 20th centuries several progresses in polymer technologies have been carried out and new fields of application have been opened, such as the pharmaceutical and biomedical ones. Synthetic and natural-based polymers have been implemented in these sectors and their applications are rapidly growing. In recent years, polymers have been used to develop devices for controlling delivery of drugs, especially acting as coatings, drug carriers and release controlling agents, or for replacing failing natural organs (Sinko, 2006). The interest in applying injection molding (IM) and micromolding (μ IM) techniques, commonly used within the plastic industry, in the pharmaceutical field is driven by the possible reduction of development and manufacturing costs. These are related to the simplification of industrial scalability, to the patentability of the new drug products and to the remarkable versatility in terms of size and shape (small and precise details in the range of micrometer included). The possibility of exploiting IM technology in the pharmaceutical field for the manufacturing of drug products has been lately considered (Zema et al., 2012).

The research activity of the Laboratory where I carried out my PhD is focused on the development of μ IM delivery platforms in the form of capsular containers and on the evaluation of IM as an alternative technique for the continuous manufacturing of tablets. Functional containers are capsular devices consisting of two matching subunits, a cap and a body, suitable to convey different drug formulations, such as powders, pellets or granules. A capsule shell for pulsatile release, able to impart a lag phase to the delivery of its content was developed. It is based on hydroxypropyl cellulose (HPC) and was trademarked as Chronocap™ (Gazzaniga et al., 2011a, b). In addition, a gastro-resistant capsular container based on hydroxypropyl methyl cellulose acetate succinate was also prepared showing promising *in vitro* and *in vivo* results (Zema et al., 2013a, b). Since the polymeric shell acts as a barrier, the performance of such devices depends on the design, the composition and the thickness of the shell, independently on the formulation conveyed, with advantages in terms of production and regulatory issues. Moreover, also the manufacturing of tablets with potential for immediate release by means of hot-melt extrusion (HME) and IM technique was demonstrated, once again proving that polymeric materials with specific properties (soluble/disintegrating) may lead to specific performances (immediate release) (Melocchi et al., 2015). In order to explore new pharmaceutical applications of the IM manufacturing technique, increasing interest is directed towards the selection of polymeric materials adequate for withstanding the processing conditions involved. Moreover, information on the processability and thermomechanical stability of pharmaceutical polymers is required because they are still limited.

The first objective of my research activity was the evaluation of the feasibility of μ IM for the manufacturing of capsular containers intended for the extended release of the conveyed drug. This part of the work was carried out in collaboration with Dipartimento di Chimica, Materiali ed Ingegneria Chimica “Giulio Natta”, Politecnico di Milano and

Dipartimento di Ingegneria Meccanica e Industriale, Università degli Studi di Brescia. Ethylcellulose (EC), one of the pharma polymers most widely employed for the preparation of prolonged-release systems, was selected as a thermoplastic material to start an evaluation process according to research methods usually used in the context of plastics. In particular, an investigation of the thermal and rheological properties of EC and its composites, containing at least a plasticizer and a possible release modifier, was undertaken. Moreover, EC barriers mimicking those of a reservoir system for prolonged-drug release, which can be permeated by biological fluids leading to the diffusion throughout its thickness of dissolved drug molecules, were prepared by IM. The evaluation of EC moldability with different amount of plasticizer performed on simple disk-shaped specimens (screening items) and the assessment of the performance of such barriers and the effect of release modifiers on the permeability of such barriers were then carried out. Overall results are reported in Chapter I and II.

Given that the interest in the use of pharmaceutical polymers via injection molding technique is not restricted to polymers intended for the formulation of prolonged-release systems, and starting from the experience of the laboratory team with molded capsular devices, a new target of research was pursued. In the last decades, great efforts have been made to attain site-specific delivery of drugs to the colon via the oral route. Colonic delivery systems were developed based on both microbiological and time-dependent approaches. The last one exploits the relative reproducibility of the transit throughout the small intestine, reported to take 3 h (\pm 1 h SE), irrespective of size characteristics of the dosage form and feeding state of subjects (Davis, 1985; Davis et al., 1986; Gazzaniga et al., 2006). Despite of the existence of molded capsular containers based on HPC allowing for a delay of the conveyed drug, basically programmed by selecting the appropriate viscosity grade of the polymer, together with the thickness of the shell, a lot of other

promising as well as challenging swellable/erodible polymers for the time-dependent approach are left.

Enzymatically-driven drug delivery systems are based on the use of biodegradable polymers (e.g., polysaccharides) intended to be *in situ* degraded through reactions that take place selectively in the colonic region (Patel & Amin, 2011). During the final part of my PhD project I was involved in the development of capsular devices manufactured by μ IM able to combine the time-controlled and the enzyme-triggered approaches to assure the release of conveyed drugs into the colon. The new capsular platform should make up for the respective limitations of the single approaches and reduce variability of the release performance. The project was carried out in collaboration with the research group of Controlled Drug Delivery Systems and Biomaterials, and the research group of Clinical Bacteriology of the Université Lille 2 Droit et Santé, where I had the opportunity to spend seven months. Results obtained are reported in Chapter III. By virtue of the supervision of Professor Jürgen Siepmann, Professor Florence Siepmann, PhD Youness Karrouit and PhD Christel Neut, having a strong expertise in microbiota-dependent colon targeting, in-depth studies about degradation of polymers by colonic microflora were carried out. Human biological samples of patients suffering from ulcerative colitis (UC) were available thanks to a close co-operation of the Clinical Bacteriology laboratory with the unit of “Maladies de l'appareil digestif et Lambling” at the Hospital Claude Huriez in Lille.

REFERENCES

- Davis, S.S. (1985). The design of evaluation of controlled release systems for the gastrointestinal tract. *Journal of Controlled Release*, 2, 27–38.
- Davis, S.S., Hardy, J.G., & Fara, J.W. (1986). Transit of pharmaceutical dosage forms through the small intestine. *Gut*, 27, 886–892.
- Gazzaniga, A., Cerea, M., Cozzi, A., Foppoli, A., Maroni, A., & Zema, L. (2011a). A novel injection-molded capsular device for oral pulsatile delivery based on swellable/erodible polymers. *AAPS PharmSciTech*, 12, 295–303.
- Gazzaniga, A., Cerea, M., Cozzi, A., Foppoli, A., Sangalli, M.E., Tavella, G., & Zema, L. (2011b). Pharmaceutical dosage forms for time-specific drug delivery. Patent US 2011/0229530 A1.
- Gazzaniga, A., Maroni, A., Sangalli, M.E., & Zema, L. (2006). Time-controlled oral delivery systems for colon targeting. *Expert Opinion on Drug Delivery*, 3, 583–597.
- Melocchi, A., Loreti, G., Del Curto, M.D., Maroni, A., Gazzaniga, A., & Zema, L. (2015). Evaluation of hot melt extrusion and injection molding for continuous manufacturing of immediate release tablets. *Journal of Pharmaceutical Sciences*, 104, 1971–1980.
- Sinko, P.J. (2006). *Martin's Physical Pharmacy and Pharmaceutical Sciences*. 5th Edition, Philadelphia: Lippincott Williams & Wilkins.
- Zema, L., Loreti, G., Melocchi, A., Macchi, E., Del Curto, M.D., Foppoli, A., & Gazzaniga, A. (2013a). Preliminary In Vivo Evaluation of a Gastroresistant Capsular Device Prepared by Injection Molding. In *40th Annual Meeting & Exposition of the Controlled Release Society 2013 - July 21-24, Honolulu, US*.
- Zema, L., Loreti, G., Melocchi, A., Maroni, A., & Gazzaniga, A. (2012). Injection Molding and its application to drug delivery. *Journal of Controlled Release*, 159, 324–331.
- Zema, L., Loreti, G., Melocchi, A., Maroni, A., Palugan, L., & Gazzaniga, A. (2013b). Gastroresistant capsular device prepared by injection molding. *International Journal of Pharmaceutics*, 440, 264–272.

Most of the results reported in the thesis have been already disclosed, *i.e.* published, submitted for publication or presented in the form of oral and poster communications to national/international Meetings.

ARTICLES:

“Rheological characterization of ethylcellulose-based melts for pharmaceutical applications” F. Baldi, J. Ragnoli, D. Zinesi, F. Bignotti, F. Briatico-Vangosa, F. Casati, G. Loreti, A. Melocchi, L. Zema - 2016 AAPS PharmSciTech, DOI: 10.1208/s12249-016-0577-0.

“Ethylcellulose-based materials for the development of prolonged-release drug delivery systems manufactured by micromolding” F. Casati, F. Briatico-Vangosa, F. Baldi, A. Melocchi, A. Maroni, A. Gazzaniga, L. Zema - submitted for publication.

“Micromolded capsular containers for colon targeting based on the combination of time-controlled and enzyme-triggered approaches” F. Casati, Y. Karrout, F. Siepmann, J. Siepmann, L. Zema, A. Gazzaniga – draft to be submitted for publication.

ORAL COMMUNICATIONS:

“Studio di materiali polimerici per lo sviluppo di sistemi capsulari a rilascio prolungato realizzati mediante microstampaggio ad iniezione (micromolding)” F. Casati, L. Zema, A. Gazzaniga. XV Scuola Nazionale Dottorale per la formazione Avanzata in Discipline Tecnologico-Farmaceutiche, September 9-11, 2015, Fisciano, Salerno, Italy

“Development of micromolded capsular devices for colonic delivery based on a combined time/microbiological approach” F. Casati, L. Zema, A. Maroni, A. Melocchi, S. Moutaharrik A. Gazzaniga. 10th World Meeting on Pharmaceutics, Biopharmaceutics and Pharmaceutical Technology, April 4-7, 2016, Glasgow, UK.

POSTER COMMUNICATIONS:

“Valutazione delle proprietà reologiche di materiali a base di etilcellulosa per la realizzazione di drug delivery systems mediante microstampaggio ad iniezione” F. Casati, G. Loreti, F. Baldi, F. Briatico Vangosa, A. Gazzaniga, L. Zema – XIII National Rheology Congress, September 7-10, 2014, Brescia, Italy.

“Continuous manufacturing of immediate release (IR) tablets by hot melt extrusion (HME) and injection molding (IM) techniques” A. Melocchi, G. Loreti, F. Casati, M. Cerea, L. Zema, A. Gazzaniga – 2014 AAPS Annual Meeting and Exposition, November 2-6, 2014, San Diego, California, US.

“Pharmaceutical polymers for the manufacturing of a capsular delivery platform by injection molding” L. Zema, A. Melocchi, G. Loreti, F. Casati, A. Maroni, A. Gazzaniga – Fourth International Symposium Frontiers in Polymer Science 20-22 May 2015, Riva del Garda, Italy.

“Development of an investigation protocol to assess the processability of pharmaceutical polymeric materials by a micromolding press” F. Casati, G. Loreti, F. Baldi, F. Briatico Vangosa, A. Gazzaniga, L. Zema – AItUN 9° Annual Meeting 25-27 May 2015, Milano, Italy.

“Sviluppo di un protocollo d’indagine per la valutazione della processabilità mediante microstampaggio ad iniezione di materiali polimerici di grado farmaceutico” F. Casati, G. Loreti, F. Baldi, F. Briatico Vangosa, A. Gazzaniga, L. Zema – AFI, June 10-12, 2015, Rimini, Italy

“Rheological and processing behavior of polymeric materials for the micromolding of capsular delivery systems” F. Briatico Vangosa, F. Baldi, F. Casati, G. Loreti, A. Melocchi, L. Zema – Polymer Processing Society (PPS) Conference, September 21-25, 2015, Graz, Austria.

“Development of an investigation protocol to assess the processability of pharmaceutical polymeric materials by a micromolding press” F. Casati, G. Loreti, F. Baldi, F. Briatico Vangosa, A. Gazzaniga, L. Zema – 2015 AAPS Annual Meeting and Exposition, October 25-29, 2015, Orlando, Florida, US.

“Injection-molded capsules for colon targeting: combining a time-controlled and an enzyme-triggered approach”. F. Casati, Y. Karrout, F. Siepmann, J. Siepmann, L. Zema, A. Gazzaniga – 4th Congress on Innovation in Drug Delivery - Site-Specific Drug Delivery, September 25-28, 2016, Antibes Juan les Pins, France.

“High-amylose maize starch processed by injection molding for the development of colonic capsular devices”. F. Casati, Y. Karrout, F. Siepmann, J. Siepmann, L. Zema, A. Gazzaniga – 2016 AAPS Annual Meeting and Exposition, November 13-17, 2016, Denver, Colorado, US.

Annex

In the context of my PhD, focused on the application of polymeric materials, withstanding hot-processes, for the development of devices able to control delivery of drugs, I had the opportunity to work on the development of prolonged release drug delivery systems (DDSs) in the form of miniaturized matrices for ophthalmic application. This secondary research activity of my work, started before the beginning of my PhD, has been carried on during all the PhD duration and it is still ongoing. Thanks to a collaboration with the University of Pisa (research group held by Prof. Patrizia Chetoni, Dipartimento di Farmacia) having a strong expertise in ophthalmic drug delivery, the development of a matrix system intended to be surgically inserted into the posterior segment of the eye for the treatment of severe ocular pathologies such as uveitis, proliferative vitreoretinopathy and retinitis has been undertaken. Inserts based on several polymers and containing 3% of a synthetic corticosteroid, fluocinolone acetonide (FA), were prepared, firstly via hot-melt extrusion (HME). From this preliminary screening of materials, a few polymers were selected: hydroxypropyl cellulose (HPC), high amylose maize starch (Amylo) and corn starch (CS). The behavior of inserts in contact with isotonic buffered saline was considered. Devices prepared with HPC and CS were too swollen to be maintained *in situ* for long periods of time; on the contrary, no substantial changes over 12 days were observed for inserts prepared with Amylo, and potential for sustained drug

release was highlighted by *in vitro* release studies. Moreover, no alteration of the release performance was seen after gamma-ray sterilization of the insert.

Thanks to these promising results, the selected formulation was processed also by injection molding (IM) technique, which would allow to properly obtain the miniaturized shape required. Firstly, screening specimens were manufactured for preliminary evaluation of molded material performances. A comparison between the two techniques (HME and IM) is being carried out in terms of intravitreal insert manufacturing, evaluating the technological characteristics, potential ocular tolerability and drug release performance of the manufactured inserts prepared with the formulation based on high-amylose maize starch.

The initial results have been gathered in a conference proceeding:

“Hot-Melt Extrusion technique (HME) to develop intravitreal inserts.” D. Monti, E. Terreni, P. Chetoni, S. Burgalassi, S. Tampucci, A. Maroni, F. Casati, L. Zema, A. Gazzaniga. 12th ISOPT Clinical, July 9-12, 2015, Berlin, Germany.

Chapter I

The contents of this chapter have already been published:

Baldi, F., Ragnoli, J., Zinesi, D., Bignotti, F., Briatico-Vangosa, F., Casati, F., Loreti, G., Melocchi, A. & Zema, L. (2016). Rheological characterization of ethylcellulose-based melts for pharmaceutical applications. *AAPS PharmSciTech*.
<http://doi.org/10.1208/s12249-016-0577-0>.

Rheological characterization of ethylcellulose-based melts for pharmaceutical applications

INTRODUCTION

Well-established techniques used to process thermoplastic polymers, such as extrusion and injection moulding (IM), have gained over the years considerable interest in the pharmaceutical field, as the number of papers recently published in the scientific literature and of drug products already on the market demonstrate (Lang et al., 2014; Repka et al., 2012; Zema et al., 2012). In some applications, considering the weight, dimensions, or dimension tolerances of molded parts, the manufacturing process should be regarded as micro-injection moulding (μ IM) rather than IM. Several advantages have been highlighted with respect to the use of IM techniques for pharmaceutical production. These are mainly relevant to the improvement of manufacturing (cost-effective and eco-friendly processes, scalability, suitability for continuous manufacturing) and technological/biopharmaceutical aspects (versatility of the product design, patentability, achievement of solid molecular dispersions/solutions of the active ingredient) (Shah et al., 2013). Functional containers, namely gastroresistant and pulsatile-release capsular devices, were lately prepared by μ IM starting from polymers with peculiar properties, *i.e.* solubility at $\text{pH} > 5.5$ and erosion/dissolution after swelling, respectively (Claeys et al., 2013; Gazzaniga et al., 2011; Zema et al., 2013b). For drug delivery purposes it would also be interesting to develop new polymeric materials intended for the manufacturing by μ IM of prolonged-release capsular devices able to slowly release their contents over 12-24 h after oral administration.

On the other hand, limitations may arise from processing pharma-grade materials, in consideration of their rheological/thermomechanical behaviour in the melt state and of

their thermal or chemical stability. Moreover, issues may be associated with the active ingredient and the product requirements, such as drug dose, release profile, stability and compliance. In this respect, a rational design of new polymers, or of a new generation of traditional ones with improved thermal properties, has recently been attempted (*e.g.* Soluplus[®], AffiniSol[™]) (Aho et al., 2015). Therefore, the need for a thorough understanding of the thermal and rheological properties of pharma-grade polymeric melts and of their impact on both processing conditions and physico-mechanical stability of the final products becomes of utmost importance (Zema et al., 2013a).

Based on such premises, the aim of this work was to investigate the rheological behaviour of melts based on ethylcellulose (EC), chosen because it is the most widely employed polymer for the preparation of prolonged drug delivery systems and, moreover, has already been processed in the molten state (Bar-Shalom et al., 2003; Quinten et al., 2009, 2011). Both neat and plasticized EC was studied. The plasticizer used was triethyl citrate, the relevant effectiveness as a processing aid for EC-based materials being known from the literature (Maru et al., 2011). Besides, as preliminary experiments showed that these materials would fail to yield the pursued release performance, two permeability modifiers (a soluble and a swellable polymer) were added to plasticized EC, based on their ability to create pores in the insoluble capsule wall. The rheological behaviour of these systems, which at processing temperatures consisted of suspensions of solid particles in the plasticized EC melt, was then evaluated. The characterization of the EC-based melts was carried out by both capillary and rotational rheometry. Capillary rheometry was employed to study the processability of the materials in view of their μ IM, whereas rotational rheometry experiments were performed to gain a more in-depth understanding of the viscoelastic response.

MATERIALS AND METHODS

Materials

Ethylcellulose, EC (Ethocel™ Std. 100 premium; Dow, United States); triethyl citrate, TEC (Aldrich, Germany); KIR (Kollicoat® IR; BASF, Germany); low-substituted hydroxypropyl cellulose, LHPC (L-HPC NBD 020; Shin-Etsu, Japan).

Methods

The following EC-based materials were prepared:

- plasticized EC (pEC): EC powder was placed in a mortar and the liquid plasticizer, TEC (20% by weight on the dry polymer), was manually added under hard mixing. The kneaded product was left stand at least 12 h at room temperature ($21 \pm 5^\circ\text{C}$, $55 \pm 5\%$ RH) before it was ground by means of a blade mill (La moulinette, Moulinex®, SEB, France).
- pEC filled with KIR or LHPC particles (pEC/KIR and pEC/LHPC, respectively): KIR powder ($d_{50} = 23 \mu\text{m}$; $d_{90} = 55 \mu\text{m}$) or LHPC powder ($d_{50} = 46 \mu\text{m}$; $d_{90} = 129 \mu\text{m}$), previously desiccated at 40°C in an oven for 24 hours, were mixed in a mortar with pEC in a 3:7 weight ratio. The mixed powders were then stored into bags under vacuum, and characterized within one or two days.

Thermal characterization

Thermal analysis on EC and pEC powders was performed on a calorimeter DSC1 STAR by Mettler Toledo (Switzerland), using nitrogen as a purge gas (70 ml/min). Indium was used as a calibration standard. Samples of about 10 mg were heated in aluminum crucibles from 30 to 200°C , maintained at this temperature for 1 min, cooled down to 30°C and reheated up to 200°C . Both heating and cooling steps were carried out at $5^\circ\text{C}/\text{min}$.

Capillary rheometry experiments

The tests were performed on a capillary rheometer Rheologic 5000 by Instron CEAST (Italy). In this instrument, the flow rate is imposed by a piston and the extrusion pressure monitored by a melt pressure transducer (data recorded every 0.15 s) placed in the barrel at a distance of 15 mm from the die entry plane; a schematic of a piston velocity-controlled capillary rheometer is reported in Figure 1a. Preliminary trials were carried out on EC to find suitable test conditions. Long residence times in the melt state promoted chemical degradation processes accompanied by gas formation. As such processes were thermally activated, the maximum test temperature was set at 180°C. 175°C was selected as the reference test temperature; additional tests were carried out at: 165, 170 and 180°C on EC; 150, 165 and 170°C on pEC; 150 and 160°C on pEC/KIR and pEC/LHPC. EC could not be examined under 165°C due to the high viscosity of the melt. Flat entrance circular dies made from Vanadis 30TM steel were employed. A die with diameter, d , of 2 mm and length to diameter ratio, l/d , of 10 was used with all the materials. Additional dies were employed, at 175°C, for: *i*) the investigation of wall slip effects, on pEC-based systems; *ii*) the determination of die entrance pressure losses, on EC and pEC. More in detail, the additional dies were: with reference to *i*), a die having $d = 1$ mm and $l/d = 10$; with reference to *ii*), dies having $d = 2$ mm and $l/d = 5$ and 20, for EC analysis, and a die having $d = 1$ mm and $l/d = 20$, for pEC analysis. A barrel with diameter, D , of 15 mm was employed. The apparent shear rate at the die wall, $\dot{\gamma}_{app,w}$, ranged between 17.8 and 560 s⁻¹ (with five different levels of $\dot{\gamma}_{app,w}$ per decade, equally spaced on a logarithmic scale, examined from the lowest to the highest). $\dot{\gamma}_{app,w}$ is related to the imposed flow rate, Q , and the die diameter, d , as follows:

$$\dot{\gamma}_{\text{app,w}} = \frac{32 \cdot Q}{\pi \cdot d^3} \quad (1)$$

Shear rates lower than 17.8 s^{-1} were not considered because time to the attainment of the steady-state would have been too long and degradation phenomena could occur. The tests at 175°C with $l/d = 10$ and $d = 1 \text{ mm}$ or 2 mm dies were carried out at least three times to check repeatability.

In every test performed, the material, after being loaded into the instrument barrel, was subjected to a pre-heating step over 420 s , under a maximum compacting force of 300 N .

All tests with the 2 mm diameter dies were conducted in such a way that the various melts experienced the same pre-fixed flow-history, in consideration of the possibility that the materials underwent residence time-controlled chemical processes while in the melt state.

More in detail, the period of time during which a material was subjected to a specific

$\dot{\gamma}_{\text{app,w}}$ (step) was fixed. Preliminary tests allowed to set the duration of each step (Δt_{step}), chosen in such a way as to guarantee the reaching of flow conditions which could be considered representative of a steady-state for every material, at the different test conditions (temperatures and, for EC, also die lengths). Δt_{step} varied between 12 and 20 s , at the highest and the lowest $\dot{\gamma}_{\text{app,w}}$ explored, respectively. With l/d fixed, in a 1 mm die

test Δt_{step} had to be higher than in a 2 mm die test, at a given $\dot{\gamma}_{\text{app,w}}$, due to the lower absolute time scale of the compression process experienced by the melt in the reservoir (with a 1 mm die the fluid is forced to enter into the capillary with a flow rate that is one eighth of the flow rate used with a 2 mm die).

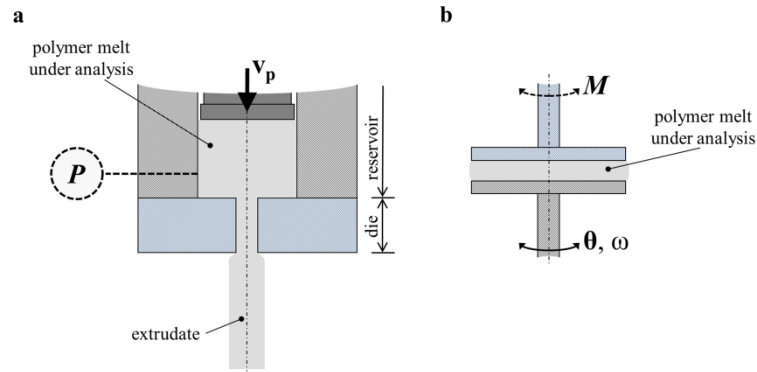


Figure 1. Schematic of (a) a capillary rheometer (piston velocity-controlled) and (b) a rotational rheometer with parallel-plate geometry (strain-controlled, for oscillatory shear measurement). With reference to (a): v_p , piston velocity; P , resulting pressure in the reservoir. With reference to (b): θ , angular displacement; ω , oscillation frequency; M , resulting torque.

Rotational rheometry experiments

Measurements of the linear viscoelastic properties were carried out using the strain-controlled rheometer ARES G2 by TA Instruments (Unites States). Dynamic frequency sweep experiments under low amplitude (2%) oscillations were carried out with a parallel-plate geometry; a schematic of a strain-controlled rotational rheometer with parallel-plate geometry, for oscillatory shear measurement, is reported in Figure 1b. The diameter of the plates was 25 mm, and the gap was set between 1.3 and 1.8 mm. Preliminary experiments, carried out to identify the adequate test conditions, put in evidence that the results were generally dependent on the overall duration of the test (practically determined by the lower limit of the frequency range explored). This should be attributed to chemical degradation processes, the impact of which is expected to increase with the residence time. Thus, the lower limit of the frequency range explored was set at a relatively high value (10 rad/s). Frequency ranged from 10 to 500 rad/s; ten different frequencies, equally spaced on a logarithmic scale (except 500 rad/s), were examined from the lowest to the highest. The

tests were performed on EC at four different temperatures, equally spaced between 160 and 175°C, and on the pEC-based systems, at six different temperatures, equally spaced between 150 and 175°C. Each test was carried out three times at each temperature, to check repeatability.

The materials were placed on the rheometer in the form of disks, with diameter of 25 mm, prepared *via* compression moulding on a P200E press by Collin (Germany). During the compression operation, the material was maintained for 280 s under the pressure of 32 bar, at 183°C for EC and 145°C for the pEC-based systems.

Scanning Electron Microscopy, SEM, analyses

SEM analyses were carried out both on KIR and LHPC powders, and on the fracture surfaces of the extrudates of the filled pEC-based materials, obtained with the tests at the capillary rheometer.

With reference to the analyses on the powders, these were carried out on gold coated powders in a scanning electron microscope (model Zeiss Evo 50 EP) operated in high vacuum mode.

With reference to the analyses on the extrudates, for each material examined, a portion of the extruded filament was collected at the exit from the rheometer die during an experiment at 175°C, with the 2 mm die with $l/d = 10$, at a $\dot{\gamma}_{app,w}$ of 100 s^{-1} . The filament was then broken under liquid nitrogen, in such a way to obtain a fracture surface almost perpendicular to the direction of the flow in the capillary, and the cryo-fractured surface was observed by a scanning electron microscope (model LEO EVO 40). The surface, prior to be analysed, was sputtered with a thin layer of gold.

RESULTS AND DISCUSSION

Thermal response

Figure 2 shows the thermograms of EC and pEC obtained from the first and the second heating scan, respectively. EC exhibits an endothermic peak, close to 190°C, whereas a similar endothermic peak was not observed in pEC heating scans. This endothermic peak, which was observed in both heating scans and thus related to a reversible thermal process, may be ascribed to the melting of high order (crystalline) domains, as suggested by Davidivich-Pinhas et al. (2014) with respect to the same EC grade. This would indicate that EC has a semi-crystalline nature that it maintains up to around 190°C. Interestingly, based on the absence of this endothermic peak in the pEC trace, it could be inferred that plasticization with TEC makes the polymer amorphous. The glass transition of EC was clearly detected in the second heating scan only (glass transition temperature, T_g , around 130°C), because the thermal response in the first heating scan was complicated by the very broad peak around 100°C probably relevant to water evaporation. A similar broad peak was found also in the first heating thermogram of pEC, the glass transition of which could not be identified even in the second heating scan.

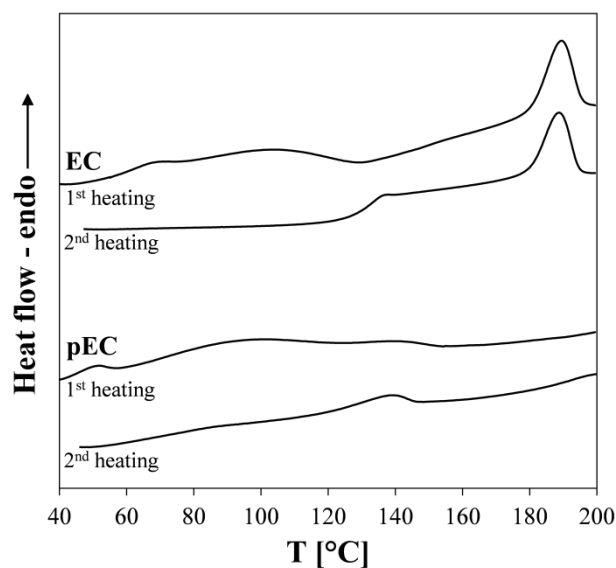


Figure 2. DSC traces of EC and pEC obtained from the first and the second heating scans (thermograms vertically shifted for clarity).

Capillary rheometry experiments

Extrudate appearance

Following rheometry tests on the EC melt, defect-free (at a macroscopic scale) extrudates were always obtained, except at the highest $\dot{\gamma}_{app,w}$ explored (that is 560 s^{-1}). At this apparent shear rate, the presence of bubbles of size comparable to the extrudate cross-section was noticed, irrespective of the working temperature. The formation of these bubbles, observed for the melt that stayed longer in the reservoir of the rheometer ($\dot{\gamma}_{app,w}$ of 560 s^{-1} corresponds to the highest residence time in the rheometer), might be explained as the consequence of chemical degradation processes (Lai et al., 2010). This was supported by results obtained from infrared spectroscopy analyses (data not reported).

pEC melt showed two distinct flow regimes within the range of $\dot{\gamma}_{app,w}$ explored in the tests carried out between 165 and 175°C: *i*) a stable steady flow regime, at low levels of $\dot{\gamma}_{app,w}$,

and *ii*) an unstable flow regime characterized by the occurrence of melt fracture phenomena, at high levels of $\dot{\gamma}_{app,w}$. The transition from the stable to the unstable regime was detected from the extrudate aspect, whereas no effects on the pressure signal trend occurred. The extrudate from the former regime appeared undistorted, appreciably transparent and with a relatively smooth surface. In the unstable regime, a highly deformed and semi-transparent extrudate, characterized by regular wavy distortions with a typical length around 3 mm, was obtained. Interestingly, the level of $\dot{\gamma}_{app,w}$ at the onset of melt fracture decreased by lowering the test temperature, from 560 s^{-1} at 175°C to 178 s^{-1} at 165°C . Extrudates at 150°C were different as compared to those obtained at higher temperatures (distortions were in general more irregular and less marked) and appeared deformed in the whole range of $\dot{\gamma}_{app,w}$ explored.

With pEC/KIR and pEC/LHPC melts, at the highest $\dot{\gamma}_{app,w}$ explored (that is 560 s^{-1}), large amplitude fluctuations in the pressure signal were recorded and acceptable steady-state extrusion pressure data could not be measured. Fluctuations could not be ascribed to the occurrence of melt fracture phenomena, since no flow instability could be recognized, and the processes at the basis of their origin are not clear. Due to the presence of the KIR and LHPC particles, the extrudate appeared opaque and with a considerably rough surface. Figures 3a and b show SEM images of these particles. KIR particles have pseudo-spherical shape and smooth surface, whereas LHPC particles appear as flakes or short fibres with rough surface. Figures 3c and d show higher magnification SEM images of the fracture surfaces obtained from the pEC/KIR and pEC/LHPC extrudate, respectively. It is worth underlining that both KIR and LHPC particles maintained their solid state at the test temperatures. LHPC particles appear better wetted by the polymer with respect to KIR

ones. SEM images of the same surfaces at lower magnification (data not reported) showed that both types of particles are uniformly dispersed within the polymeric matrix.

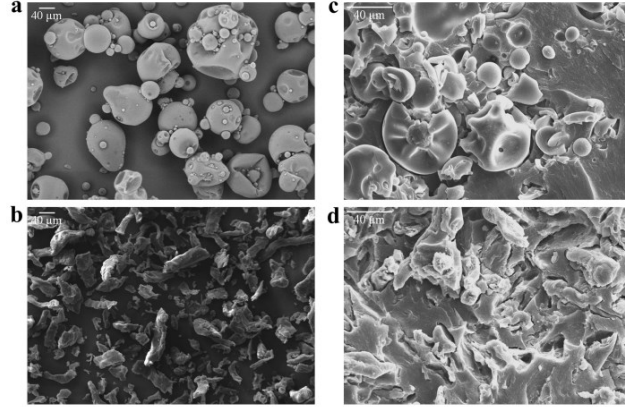


Figure 3. SEM images of (a) KIR and (b) LHPC particles, and of cryo-fracture surfaces obtained from the extrudates of (c) pEC/KIR and (d) pEC/LHPC.

Apparent viscosity functions

Figures 4a-d show the steady-state apparent shear viscosity, η_{app} , vs apparent shear rate at the die wall, $\dot{\gamma}_{app,w}$, curves obtained for EC and the pEC-based melts at different temperatures and with the die having $d = 2$ mm and $l/d = 10$. At a given $\dot{\gamma}_{app,w}$, η_{app} is evaluated as the ratio between the apparent shear stress at the die wall, $\tau_{app,w}$, and $\dot{\gamma}_{app,w}$, with $\tau_{app,w}$ calculated from the steady-state extrusion pressure, ΔP , uncorrected for the die entrance pressure drop, ΔP_{ent} , as:

$$\tau_{app,w} = \frac{\Delta P}{4 \cdot l/d} \quad (2)$$

Data at 175°C are the average of three replicated measures (bars in figure represent the standard deviation; when not visible, they are shorter than the symbol height). Working

with EC at 165°C, $\dot{\gamma}_{\text{app,w}}$ higher than 178 s⁻¹ could not be determined since extrusion pressure exceeded the maximum capacity of the pressure transducer (50 MPa). Data indicated with open or thinner symbols and connected by dotted segments should be regarded as critical since melt fracture occurred (for pEC) or acceptable values of steady-state extrusion pressure could not be detected (for EC and filled pEC-based melts, at $\dot{\gamma}_{\text{app,w}} = 560 \text{ s}^{-1}$).

The pronounced effect of the test temperature on the viscosity of EC melt is clearly shown in Figure 4a. Under the assumption that the relationship between ΔP_{ent} and the true shear stress at the die wall, τ_w , is temperature invariant (Laun & Schuch, 1989), the time-temperature superposition principle was tentatively applied to the $\tau_{\text{app,w}}$ data obtained. Each logarithmic plot of $\tau_{\text{app,w}}$ vs $\dot{\gamma}_{\text{app,w}}$ referred to a specific temperature, T , was horizontally shifted to overlap as much as possible the reference curve at $T_0 = 175^\circ\text{C}$. Such a procedure permitted to evaluate, for each temperature, the shift factor, a_T , at constant $\tau_{\text{app,w}}$, averaged over the shear stress range explored. Good results with respect to the overlapping were generally obtained, and the shift factor turned out practically independent from the stress level within the whole shear stress range explored. This appears rather surprising taking into account the complex evolving micro-structure of the EC melt.

An Arrhenius type dependence on temperature was observed for a_T , and a viscous flow activation energy, $E_{0,s}$, of $\approx 240 \text{ kJ/mol}$ was obtained (see Laun & Schuch, 1989, for Arrhenius equation) – the subscript “s” is used in $E_{0,s}$ to indicate that the activation energy is derived from steady-state flow properties. By considering that, for an ordinary industrial polymer melt, the viscous flow activation energy derived from fully developed flow tests is of the order of a few tens of kJ/mol and typically keeps smaller than 100 kJ/mol (Baldi et al., 2009; Laun 1984), the value of $E_{0,s}$ obtained for EC seems very high. The pronounced

sensitivity of apparent viscosity to temperature could be related to the thermal response of EC. Due to the tendency to undergo chemical degradation processes at high temperatures, the test temperatures have been kept relatively low, just below the endothermic peak ascribed to the melting of the crystalline domains (see *Thermal response* section). At the test temperatures, EC melt is expected to have a heterogeneous microstructure with high order regions dispersed within an amorphous matrix and, therefore, it can be argued that small temperature variations can induce substantial changes in the material microstructure and in polymer chains mobility. These temperature-induced microstructural modifications are likely to be reflected in the viscous response obtained in the capillary rheometer, which varied widely with temperature. A contribution of thermally activated chemical processes occurring during the rheometry test, which could reduce the length of the polymeric chains and, therefore, the viscosity of the material, could not be ruled out. It is worth noting that the phenomena described above do not explain the “apparent thermorheological simplicity” observed for EC. A comprehensive analysis of the processes that govern the temperature dependence of the viscosity here observed would require an extensive work aimed at studying the chemical-physical processes undergone by EC during a capillary rheometer test, and it could be a matter of further studies.

From a_T data, the η_{app} vs $\dot{\gamma}_{app,w}$ master curve of EC was constructed at $T_0 = 175^\circ\text{C}$ (data at 560 s^{-1} have been removed). In Figure 4a, shifted data-points [$(\dot{\gamma}_{app,w} \cdot a_T; \eta_{app}/a_T)$ where a_T is temperature shift factor] are indicated with grey symbols, and dashed line is sketched as a guideline for the eye. The EC melt shows a non-Newtonian behaviour, apparently shear-thinning, but different from that of an ordinary polymer melt. It is characterized by a threshold level of apparent viscosity, $\eta_{app,\infty}$ ($\eta_{app,\infty} \approx 670\text{ Pa}\cdot\text{s}$), approached at high shear rates. This behaviour recalls that of Bingham fluids (Larson, 1999), even if in this case the

existence of a yield stress cannot be firmly stated on the basis of the data obtained. The presence of a threshold at a relatively high level of viscosity clearly indicates that EC can be very hardly processed *via* μ IM, at least at process temperatures compatible with its chemical stability. This was confirmed by explorative μ IM tests, performed with a μ IM press (BabyPlast 6/10P; Cronoplast S.L., Barcelona, Spain) equipped with a disk-shaped screening mould (the details of machine and mould used are reported in (Zema et al., 2013a)). At process temperatures comparable with those used in the capillary rheometer tests, EC could not be processed if un-plasticized.

For comparison purposes, the flow curve (master curve at $T_0 = 175^\circ\text{C}$) of EC is also reported in Figures 4b-d relevant to pEC-based melts. From Figure 4b it can be observed that the plasticization with TEC makes the rheological response of pEC consistent with that of an ordinary polymer melt. The trend of the flow curve does not indicate the existence of a threshold level of apparent viscosity and, at the highest $\dot{\gamma}_{\text{app,w}}$ explored, η_{app} of pEC is remarkably lower than that of EC (at 175°C). This suggests for the pEC melt the possibility to be processed *via* μ IM. By comparing the flow curves of pEC/KIR and pEC/LHPC, reported in Figures 4c and d, respectively, with that of pEC, it emerges that the presence of a secondary phase in pEC, either KIR or LHPC particles, promotes an increase in η_{app} , at a given level of $\dot{\gamma}_{\text{app,w}}$, without impairing the shear-thinning nature of the response, and therefore the potential for the material to be processed at high shear rates. Also these assumptions were confirmed by preliminary μ IM trials performed as above described.

As shown in Figures 4b-d, the test temperature leaves the apparent viscosity function of pEC-based melts practically unchanged. This seems to suggest that the flow of these materials is not governed by the shear viscosity of the melt, and that a more complex flow

takes place. Moreover, for unfilled pEC the test temperature was already shown to influence the level of $\dot{\gamma}_{app,w}$ at the onset of melt fracture phenomena (see *Extrudate appearance* section), which are generally related to a complex equilibrium between adhesion and slip of the polymer melt at the wall metal interface (Hatzikiriakos & Dealy, 1992b; Piau et al., 1995). As polymer/wall interface processes can play a role in defining the capillary flow of the pEC-based melts, the occurrence of wall slip effects in the capillary flow of these melts was verified.

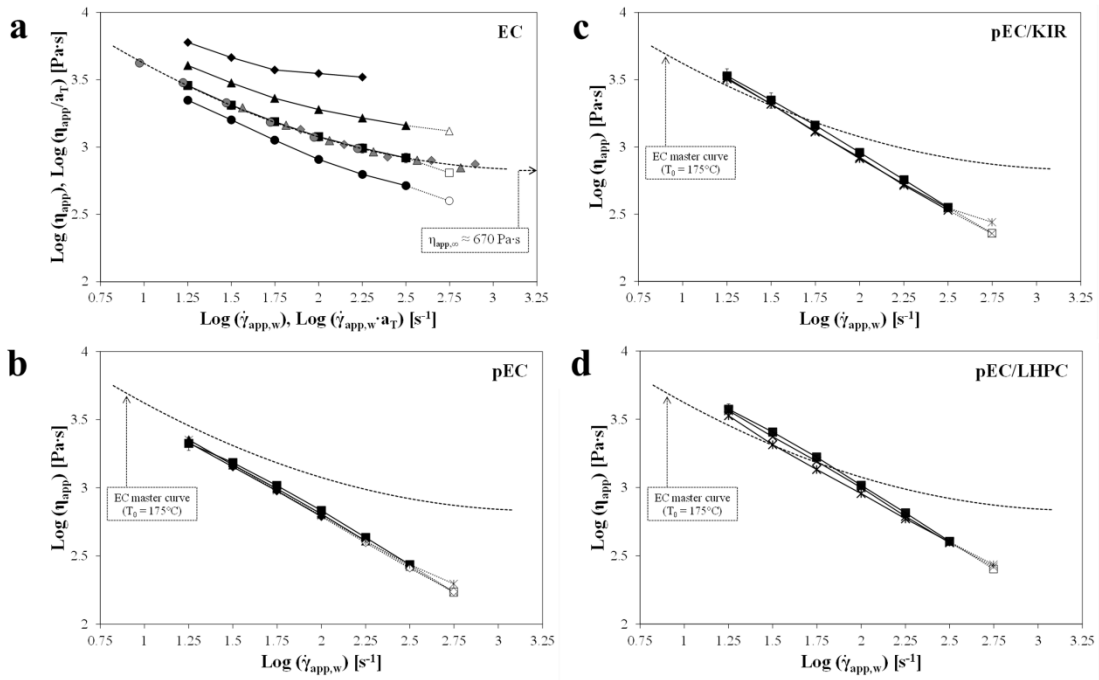


Figure 4. Steady-state apparent shear viscosity, η_{app} , vs apparent shear rate at die wall, $\dot{\gamma}_{app,w}$, for (a) EC, (b) pEC, (c) pEC/KIR, (d) pEC/LHPC, from capillary rheometry tests at: 180°C, *circle* (a); 175°C, *square* (a-d); 170°C, *triangle* (a,b); 165°C, *rhomb* (a,b); 160°C, “*×*” (c,d); 150°C, *asterisk* (b-d).

Wall slip effects were studied by the application of the Mooney technique (Mooney, 1931). This approach assumes that the fluid is homogeneous and the slip velocity at the die wall, v_s , is a function of the wall shear stress, τ_w , only. The apparent shear rate at the die wall,

$\dot{\gamma}_{app,w}$, which the polymer melt is subjected to during capillary flow at a given τ_w , results from: (i.) a purely viscous bulk contribution, $\dot{\gamma}_{app,w,v}$, that would only depend on the intrinsic behaviour of the material, and (ii.) a wall slip contribution, $\dot{\gamma}_{app,w,s}$, that depends on v_s and die diameter, d , according to Eq. 3:

$$\dot{\gamma}_{app,w,s} = \frac{8}{d} \cdot v_s(\tau_w) \quad (3)$$

Tests with different die diameters are carried out and τ_w vs $\dot{\gamma}_{app,w}$ curves are obtained. v_s and $\dot{\gamma}_{app,w,v}$ can thus be determined from the slope and the intercept, respectively, of the least square regression straight line that interpolates the $\dot{\gamma}_{app,w}$ vs $1/d$ data (Mooney plot), at a given level of τ_w . In this work, under the assumption that ΔP_{ent} , do not significantly change with the die diameter (supported by the experimental observation that for pEC the levels of ΔP_{ent} measured with the highest contraction ratio, D/d , available are very small, as shown below, in the *Entrance pressure losses* section), extrusion pressure data uncorrected for ΔP_{ent} were used, and $\tau_{app,w}$ rather than τ_w data were employed. By considering that slip phenomena can depend in principle also on the extrusion pressure (Hatzikiriakos & Dealy, 1992a), the dies for wall slip analysis were chosen in such a way that similar levels of steady-state extrusion pressure were reached in the experiments. More specifically, data from tests carried out, at 175°C, with dies having different diameter ($d = 1$ and 2 mm) but same l/d ($l/d = 10$) were used. In Figure 5 the $\tau_{app,w}$ vs $\dot{\gamma}_{app,w}$ curves obtained with the two different dies for pEC, pEC/KIR and pEC/LHPC are compared (bars in figure represent the standard deviation; when not visible, they are shorter than the symbol height). The data obtained with the 2 mm die at 560 s⁻¹ were not taken into account; for pEC, also the datum obtained with the 1 mm die at 560 s⁻¹ was omitted since melt fracture was observed. The

curve obtained with the 2 mm die is above the 1 mm die curve over the whole range of $\dot{\gamma}_{app,w}$, independent of the material, thus indicating that slip effects occur. It is worth noting that, contrary to what generally observed for melts based on ordinary polymeric materials exhibiting wall slip in capillary flow (Hatzikiriakos & Dealy, 1992a), at the highest levels of $\tau_{app,w}$ (that is of ΔP) the curves obtained with the different dies tend to get closer. For pEC, they even overlap at the highest $\dot{\gamma}_{app,w}$, indicating that, for this material, high levels of ΔP , close to the onset of melt fracture phenomena, lead to slipping suppression. Considering that (i.) $\dot{\gamma}_{app,w}$ data from the curves obtained with the two different die diameters, at a given $\tau_{app,w}$, refer to different residence times in the rheometer (longer for the 1 mm die), and that (ii.) the linearity of the Mooney plot, corresponding to a given $\tau_{app,w}$, could not be proven since only two diameters were used, only slip velocity was determined and referred to as an “apparent slip velocity” (indicated with $v_{s,app}$).

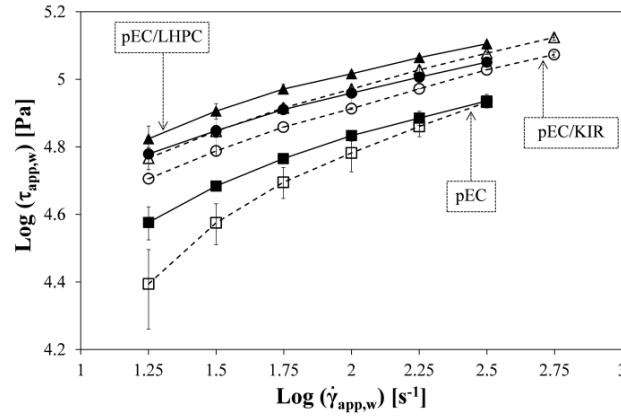


Figure 5. Apparent shear stress at the die wall, $\tau_{app,w}$, as a function of the apparent shear rate at the die wall, $\dot{\gamma}_{app,w}$, for pEC (*square*), pEC/KIR (*circle*), pEC/LHPC (*triangle*), from capillary rheometry tests at 175°C, with $d = 2$ mm (full symbols) and $d = 1$ mm (open symbols).

In Figure 6, $v_{s,app}$ is reported as a function of $\tau_{app,w}$ for pEC and the filled pEC-based systems, in a double-logarithmic plot. For pEC, the downward arrow indicates the tendency of slipping phenomena to be suppressed at high levels of $\tau_{app,w}$. As the dependence of $v_{s,app}$ on $\tau_{app,w}$ within the explored range of $\tau_{app,w}$ appeared of power-law-type (linear in a double-logarithmic plot), as for ordinary polymer melts, with particular reference to polyolefins (Hatzikiriakos & Dealy, 1992a; Laun, 2004), data were accordingly fitted.

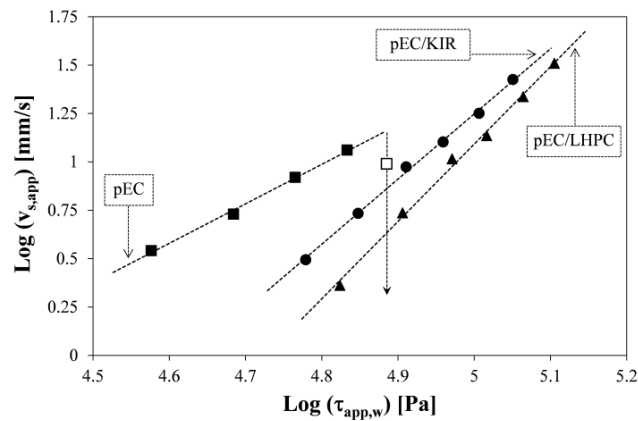


Figure 6. “Apparent wall slip velocity”, $v_{s,app}$, as a function of the apparent shear stress at the die wall, $\tau_{app,w}$, for pEC (*square*), pEC/KIR (*circle*), pEC/LHPC (*triangle*), from capillary rheometry tests at 175°C.

In Fig. 6, power-law fitting curve (dashed line) is traced for each series of data (for pEC the point at $\tau_{app,w} = 76770$ Pa, indicated with an open symbol, was not included in the fitting). The order of magnitude of the slip velocity obtained for the pEC-melts is comparable with that of polyolefin-based melts, but the levels of shear stress at which wall slip phenomena occur are generally lower (Hatzikiriakos & Dealy, 1992a; Haworth & Khan, 2005). With respect to the unfilled pEC, the presence of a secondary phase, in pEC/KIR and pEC/LHPC, promotes a decrease in $v_{s,app}$, at a given level of $\tau_{app,w}$, but enlarges the $\tau_{app,w}$ range of slip, allowing high values of $v_{s,app}$ to be reached. This latter effect is due to the different sensitivity of $v_{s,app}$ on $\tau_{app,w}$, exhibited by pEC and the filled

pEC-based melts, here represented by the slope of the power-law fitting line (that is 2.0 for pEC, 3.4 and 4.0 for pEC/KIR and pEC/LHPC, respectively). Most of the flow occurs by wall slip, and the slip contribution to the flow rate decreases by increasing the shear stress level; at the lowest level of $\tau_{app,w}$, for the capillary with the highest surface/volume ratio (that is the 1 mm die), it is approximately the 90, 80 and 70% of the imposed flow rate for pEC, pEC/KIR and pEC/LHPC melt, respectively. It can be thought that the pronounced wall slip effects of pEC-based melts are due to the presence of the plasticizer, TEC, which, during the capillary flow, could migrate at the die wall. This hypothesis should be confirmed with specific analyses, which could be a matter of further studies.

Entrance pressure losses

Figures 7a and b show Bagley plots constructed from the steady-state extrusion pressure, ΔP , data measured at various $\dot{\gamma}_{app,w}$, at 175°C, for EC and pEC, respectively; for EC, ΔP data were measured in tests carried out with dies having diameter of 2 mm (data at 560 s⁻¹ were not included in the analysis) whereas, for pEC, in tests with 1 mm dies. At $l/d = 10$, each datum is the average of three values measured in replicated experiments (standard deviation bars indicated).

In Bagley plot, the experimental (l/d ; ΔP) data at a given $\dot{\gamma}_{app,w}$ typically lie on a straight line, and ΔP_{ent} value is determined by extrapolating to zero the least square regression line that interpolates them. From Fig. 7a, it clearly emerges that, for EC, at each level of $\dot{\gamma}_{app,w}$ explored, the dependence of ΔP on the die length to diameter ratio, l/d , is not linear. This curvature of the Bagley plots cannot be related to the effect of pressure on viscosity, nor to slipping phenomena, since these factors would induce an upward shift of curves (Hatzikiriakos & Dealy, 1992a); it rather might be ascribed, at least for the highest levels

of $\dot{\gamma}_{app,w}$, to viscous heating effects, mainly occurring in the longest die (that is the die with $l = 40$ mm), where they are expected to be more marked (Cox & Macosko, 1974; Rosenbaum & Hatzikiriakos, 1997). In support of this discussion is the observation that EC viscosity is very sensitive to temperature, and a small temperature increase produced by viscous heating can give rise to a pronounced decrease in viscosity (and therefore in ΔP). In accordance with these results, for the determination of ΔP_{ent} of EC, only data obtained with the two shorter dies (with $l/d = 5$ and 10), and indicated in Figure 7a with full symbols, were used.

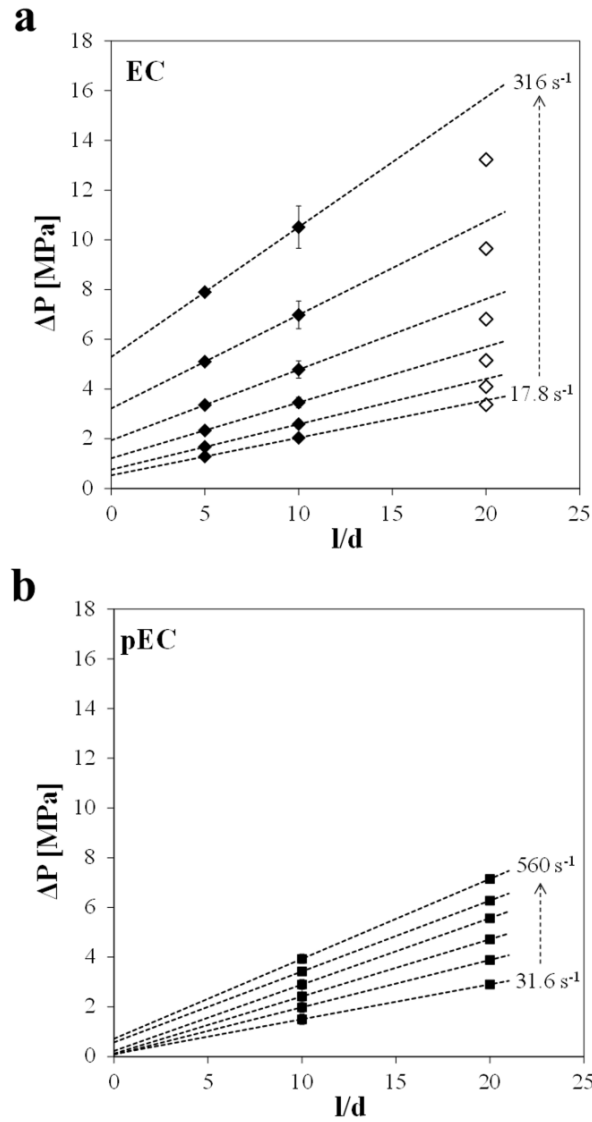


Figure 7. Bagley plots for (a) EC and (b) pEC, from capillary rheometry tests carried out with dies having $d = 2$ mm for EC (a) and $d = 1$ mm for pEC (b), at 175°C . For EC (a), data-points at $l/d = 20$ (open symbols) not used for ΔP_{ent} determination.

For the pEC melt, too small ΔP_{ent} values were obtained by applying the Bagley procedure to data from tests performed with 2 mm dies. When very small, ΔP_{ent} values can turn out comparable with the statistical error induced by the extrapolation procedure, thus becoming not reliable. Therefore, it is necessary to resort to a test flow geometry that could

induce higher level of ΔP_{ent} to be reached. By considering that at a given $\dot{\gamma}_{\text{app,w}}$, the higher the reservoir to die diameter ratio, D/d , the higher is ΔP_{ent} (with D fixed) (Baldi et al., 2014), 1 mm dies were used for ΔP_{ent} evaluation, and more reliable ΔP_{ent} data could be obtained except for the lowest $\dot{\gamma}_{\text{app,w}}$. In consideration of the fact that pEC shows wall slip phenomena that can be pressure dependent, for the determination of ΔP_{ent} only data obtained with the two shortest dies available (with $l/d = 10$ and 20) were used (Figure 7b). For both EC and pEC, at each $\dot{\gamma}_{\text{app,w}}$ examined, the value of ΔP_{ent} was determined as the intercept of the straight line traced on the two (l/d ; ΔP) valid points (dashed lines in Figures 7a and b), and, in turn, the true shear stress at the die wall, τ_w , was evaluated. Figure 7 clearly shows that the levels of ΔP_{ent} of EC are considerably higher than those of pEC (for EC, at 316 s^{-1} , ΔP_{ent} is higher than 5 MPa, whereas for pEC, at 560 s^{-1} it does not even reach 1 MPa). In Figure 8, the ratio between ΔP_{ent} and τ_w is plotted as a function of $\dot{\gamma}_{\text{app,w}}$, for both EC and pEC, and power-law fitting curve (dashed line) is traced for each series of data. It clearly emerges that, in the whole range of $\dot{\gamma}_{\text{app,w}}$, the level of $\Delta P_{\text{ent}}/\tau_w$ obtained for EC is largely higher than that obtained for pEC. By considering that, quoting Jerman and Baird (1981), “values of $\Delta P_{\text{ent}}/\tau_w$ are thought to represent the elasticity of a polymer melt”, this result indicates that plasticization with TEC considerably reduces the elastic character of EC in the melt state. This is further confirmed by the swell behaviour exhibited by the two extrudates: the diameter of the EC extrudate (evaluated after material solidification on samples obtained from tests carried out at 175°C , with the 2 mm die with $l/d = 10$) was larger than that of the pEC one. The difference between the two materials increased by increasing the level of $\dot{\gamma}_{\text{app,w}}$ undergone by the melt in the capillary flow (at 316 s^{-1} , the diameter of EC extrudate was nearly twice that of pEC). The pronounced

elastic character exhibited by the EC melt is probably another reflection, at a macroscopic scale, of its peculiar microstructure.

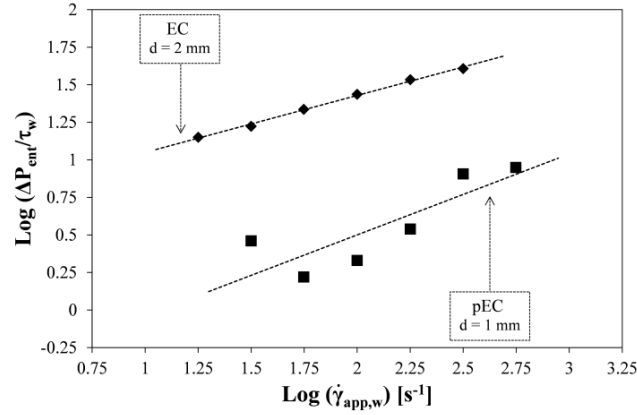


Figure 8. Ratio between the die entrance pressure drops, ΔP_{ent} , and the true shear stress at the die wall, τ_w , as a function of the apparent shear rate at the die wall, $\dot{\gamma}_{app,w}$, for EC (*rhomb*) and pEC (*square*), from capillary rheometry tests at 175°C.

Rotational rheometry experiments

Figures 9a and b show the absolute value of the complex viscosity, $|\eta^*|$, and the dynamic storage modulus, G' , vs frequency, ω , master curves of the various materials, constructed from the data obtained at the various temperatures examined (reference temperature, $T_0 = 175^\circ\text{C}$). Each datum reported in the graphs is the average of three values measured in replicated experiments (bars representing the standard deviation are not reported in the graphs as they were generally shorter than the symbol height). Differently from that observed with the capillary rheometer tests, at the rotational rheometer also for the pEC-based melts a clear effect of temperature was observed. This is probably due to the fact that the shear stress levels reached in these latter tests, remarkably lower than those reached in the capillary experiments, are insufficient to promote slip phenomena. The successful attainment of a master curve for each system examined by shifting the rheological data

with respect to frequency, on the basis of the temperature shift factors, a_T , demonstrates the validity of the time-temperature superposition principle [already demonstrated for the EC melt by referring to the capillary rheometer results (see *Capillary rheometry experiments, Apparent viscosity functions* section)]. An Arrhenius type dependence on temperature was observed for a_T , and a flow activation energy, $E_{0,d}$, was obtained for each melt – the subscript “d” is used in $E_{0,d}$ to indicate that this flow activation energy is obtained from flow properties measured in dynamic tests. $E_{0,d}$ values are reported in Table 1.

Table 1. Flow activation energies, $E_{0,d}$, of melts from dynamic tests at the rotational rheometer.

Material	$E_{0,d}$ [kJ/mol]
EC	335
pEC	120
pEC/KIR	140
pEC/LHPC	150

For the EC melt, an appreciable difference between the flow activation energy calculated from capillary and rotational rheometer tests was obtained. This difference should be related to the different mechanical histories experienced by the polymer melt in the two rheometers. $E_{0,d}$ of pEC is largely lower than that of EC. In consideration of the differences between the microstructures of these two melts (see *Thermal response* section), this result seems to support the idea that the high sensitivity to temperature exhibited by EC might be ascribed to the presence of high order domains in its melt microstructure, that were not found in the pEC melt. Finally, the incorporation of either KIR or LHPC particles in the pEC induces an increase in $E_{0,d}$.

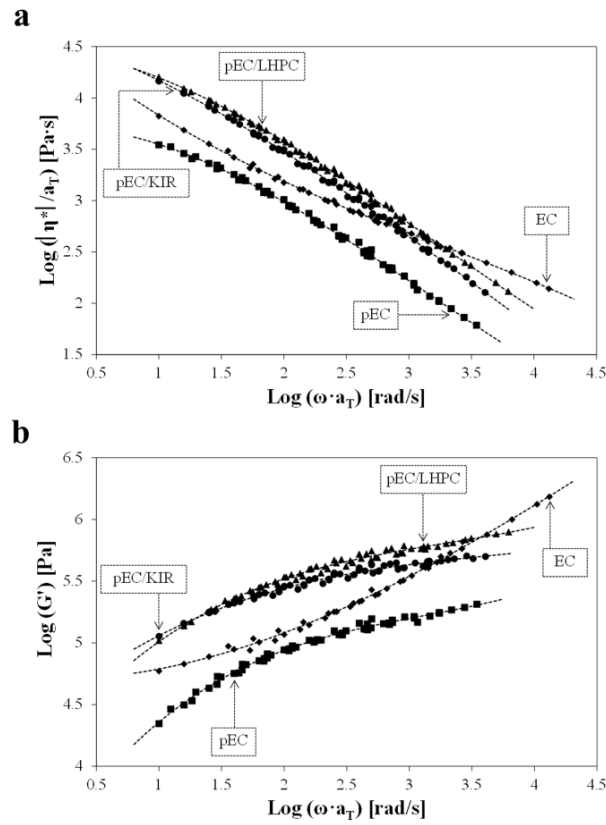


Figure 9. (a) Absolute value of the complex viscosity, $|\eta^*|$, and (b) dynamic storage modulus, G' , vs frequency, ω , master curves ($T_0 = 175^\circ\text{C}$) of EC (*rhomb*), pEC (*square*), pEC/KIR (*circle*) and pEC/LHPC (*triangle*), from rotational rheometry experiments.

From Figure 9 it emerges that the viscoelastic behaviour of the pEC-based melts is that typical of homogeneous polymer melts (Macosko, 1994). With respect to the neat pEC melt, the presence of a secondary phase in pEC/KIR and pEC/LHPC melts induces a significant increase in both G' and $|\eta^*|$, within the explored range of frequency. This result is in agreement with the effects reported in literature for polymer melts filled with rigid particles (Khan & Prud'Homme, 1987; Larson, 1999), indicating that KIR and LHPC particles enhance the capacity of the pEC melts to store elastic energy and dissipate

mechanical energy. Interestingly, LHPC particles appear the most effective in promoting an increase in both dynamic properties. By considering for pEC melt a density of 1.01 g/cm³ (measured by melt flow rate tests carried out by a Modular Melt Flow Indexer by Ceast-Instron, at 170°C, with an extruding mass of 10 kg, according to ISO 1133-1:2011), and for KIR and LHPC particles density values of 0.94 and 1.29 g/cm³, respectively (evaluated from volume and mass data collected from three compacts prepared by means of a hydraulic press equipped with flat punches), 32 and 25% of actual filler volume contents in pEC/KIR and pEC/LHPC melts were estimated. This result indicates that the higher effectiveness exhibited by LHPC particles cannot be ascribed to a higher volume content of rigid particles in the melt, but it is intrinsically associated with the nature of these particles, which differ from those of KIR in geometry, surface roughness and chemical composition. Interestingly, by considering that LHPC particles (i.) promote an increase in G' and $|\eta^*|$ that is practically independent of the frequency, and (ii.) leave the out-of-phase angle, δ ($\tan[\delta]=G''/G'$), practically unchanged (data of δ not shown here), with respect to the unfilled melt, the viscoelastic response of pEC/LHPC seems to be governed by the matrix. By contrast, for pEC/KIR melt, the frequency dependence of the dynamic properties and the values of the out-of-phase angle obtained, which are different from those of the matrix, suggest that KIR particles embedded in the polymer melt actively contribute to its viscoelastic response.

The viscoelastic behaviour of the EC melt differs considerably from that of the pEC-based melts and this might be ascribed to its particular microstructure. In Figure 10, the shear viscosity, η , obtained from capillary rheometer tests is compared with the complex viscosity, $|\eta^*|$, obtained from rotational rheometer tests (viscosity data measured at 175°C). η data are determined from data of true shear stress (corrected for ΔP_{ent}), τ_w , and true shear rate (calculated according to the Rabinowitsch–Weissenberg method (Macosko, 1994)), $\dot{\gamma}$

, both evaluated at the die wall, and are plotted as a function of $\dot{\gamma}$. It emerges that the Cox-Merz rule (Macosko, 1994), according to which an approximate agreement exists between $|\eta^*(\omega)|$ and the steady-state shear viscosity, $\eta(\dot{\gamma})$, if the angular frequency, ω in [rad/s], is set equal to the shear rate, $\dot{\gamma}$ in [s^{-1}], is not verified.

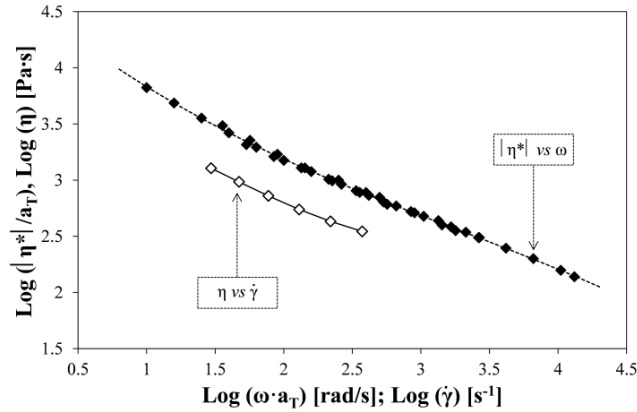


Figure 10. Steady-state shear viscosity, η , vs shear rate (at the die wall), $\dot{\gamma}$, curve from capillary rheometry tests (open symbols) compared with the absolute value of the complex viscosity, $|\eta^*|$, vs frequency, ω , master curve from rotational rheometry tests (full symbols) for EC, at 175°C.

In fact, within the range of $\dot{\gamma}$ explored, the value of $|\eta^*|$ is roughly 2.5 times that of η . Even by replotting the complex viscosity data as a function of the maximum (or “effective”) shear rate experienced in the dynamic tests, that is ω multiplied by the amplitude of the oscillation (0.02 in these experiments), as proposed for filled melts by Doraiswamy et al. (1991), steady-state and complex viscosity data do not overlap. The mechanical history experienced by the melt in the two types of rheometer is different with respect to: (i.) the type of flow (a steady-state pressure-induced shear flow in the capillary rheometer, and a dynamic drag-induced shear flow under low amplitude oscillation in the

rotational rheometer); (ii.) the residence time (a capillary rheometer test is roughly two times longer than a rotational rheometer test). In addition, the material tested at the rotational rheometer underwent a compression moulding operation prior to be tested. These differences are likely to be at the basis of the differences between viscosity and flow activation energy data obtained with the two types of test. More specifically, with reference to the viscosity, it is reasonable to think that data coming from the capillary rheometer refer to a melt characterized by a higher degree of microstructural orientation. In spite of the difference between the values of η and $|\eta^*|$, the dependence on the time-variable (either $\dot{\gamma}$ or ω) observed for the two different sets of viscosity data is similar, and may suggest that the shear-thinning characteristic of the melt is being progressively reduced as $\dot{\gamma}$ (or ω) increases. Interestingly, the trend of the viscosity function obtained from the rotational rheometer tests does not suggest the existence of a threshold viscosity for EC melt. This result seems to indicate that the threshold noted for the apparent viscosity ($\eta_{app,\infty}$ in Figure 4a), coming from capillary rheometer tests, originates in part from the high levels of die entrance pressure losses that this melt exhibits at high $\dot{\gamma}_{app,w}$ (it is worth recalling that η_{app} data were evaluated from data of apparent shear stress, $\tau_{app,w}$, uncorrected for ΔP_{ent}).

CONCLUSIONS

In this work, a rheological characterization of ethylcellulose (EC)-based melts intended to be used for the production *via* μ IM of prolonged-release capsular devices was carried out. Neat EC, EC plasticized with TEC (pEC), and pEC containing particles of either a water soluble polymer (KIR) or a hydrophilic swellable polymer (LHPC), added to enhance the permeability of the EC-based materials in view of their final use, were examined by both capillary and rotational rheometry tests.

Capillary rheometry tests showed that this peculiar melt, which is expected to have a heterogeneous microstructure with high order regions dispersed within an amorphous matrix, exhibits a non-Newtonian, apparently shear-thinning behaviour characterized by a threshold in the steady-state apparent shear viscosity, η_{app} , approached at high flow rates. The existence of this η_{app} threshold indicates that neat EC cannot be practically processed *via* μ IM. From both capillary and rotational rheometry experiments EC melt shows a very high sensitivity of viscosity to temperature.

Capillary rheometry tests suggest that plasticization with TEC makes EC (pEC) processable *via* μ IM. For the pEC melt, which has a homogeneous amorphous structure, the threshold in the η_{app} was not observed, and a η_{app} function consistent with that of an ordinary polymer melt was obtained. Plasticization with TEC considerably reduces the elastic character of EC, and fosters the occurrence of pronounced wall slip phenomena in the capillary flow. Also for the pEC melts filled with the permeability modifiers, either KIR or LHPC particles (filler volume content around 30%), most of the capillary flow occurs by wall slip. The presence of these particles in the pEC melt induces an increase in η_{app} , which however does not compromise the material shear-thinning behaviour, and therefore its processability. Rotational rheometry experiments clearly indicate that, in the frequency range explored, both LHPC and KIR particles induce an increase in both the

complex viscosity, $|\eta^*|$, and the dynamic storage modulus, G' , with LHPC particles being the most effective at promoting this increase. KIR particles seem to actively contribute to the frequency dependency of the dynamic properties, whereas the frequency response of the pEC melt filled with LHPC particles seems to be governed by the matrix.

The study performed on EC turned out to be a valuable guideline for the development of polymeric materials with potential for new pharmaceutical applications of μIM .

REFERENCES

- Aho, J., Boetker, J. P., Baldursdottir, S., & Rantanen, J. (2015). Rheology as a tool for evaluation of melt processability of innovative dosage forms. *International Journal of Pharmaceutics*, *494*, 623–642.
- Baldi, F., Franceschini, A., Bignotti, F., Tieghi, G., & Riccò, T. (2009). Rheological behaviour of nano-composites based on polyamide 6 under shear and elongational flow at high strain rates. *Rheologica Acta*, *48*, 73-88.
- Baldi, F., Ragnoli, J., & Briatico Vangosa, F. (2014). Measurement of the high rate flow properties of filled HDPE melts by capillary rheometer: Effects of the test geometry. *Polymer Testing*, *37*, 201-209.
- Bar-Shalom, D., Slot, L., Wang Lee, W., & Wilson, C.G. (2003). Development of the Egalet® technology. In Rathbone, M. J., Hadgraft, J., & Roberts, M. S. (Eds.), *Modified-release drug delivery technology* (pp. 263–271). New York: Marcel Dekker.
- Claeys, B., De Coen, R., De Geest, B.G., De La Rosa, V. R., Hoogenboom, R., Carleer, R., Adriaensens, P., Remon, J.P., & Vervaet, C. (2013). Structural modifications of polymethacrylates : Impact on thermal behavior and release characteristics of glassy solid solutions. *European Journal of Pharmaceutics and Biopharmaceutics*, *85*, 1206–1214.
- Cox, H.W., & Macosko, C.W. (1974). Viscous dissipation in die flows. *AIChE Journal*, *20*, 785-795.
- Davidivich-Pinhas, M., Barbut, S., & Marangoni, A.G. (2014). Physical structure and thermal behaviour of ethylcellulose. *Cellulose*, *21*, 3243-3255.
- Doraiswamy, D., Mujumdar, A.N., Tsao, I., Beris, A.N., Danforth, S.C., & Metzner, A.B. (1991). The Cox-Mertz rule extended: A rheological model for concentrated suspensions and other materials with a yield stress. *Journal of Rheology*, *35*, 647-685.
- Gazzaniga, A., Cerea, M., Cozzi, A., Foppoli, A., Maroni, A., & Zema, L. (2011). A novel injection-molded capsular device for oral pulsatile delivery based on swellable/erodible polymers. *AAPS PharmSciTech*, *12*, 295–303.
- Hatzikiriakos, S.G., & Dealy, J.M. (1992a). Wall slip of molten high density polyethylenes. II. Capillary rheometer studies. *Journal of Rheology*, *36*, 703-741.

- Hatzikiriakos, S.G., & Dealy, J.M. (1992b). Role of slip and fracture in the oscillating flow of HDPE in a capillary. *Journal of Rheology*, *36*, 845-884.
- Haworth, B., & Khan, S.W. (2005). Wall slip phenomena in talc-filled polypropylene compounds. *Journal of Materials Science*, *40*, 3325-3337.
- Jerman, R.E., & Baird, D.G. (1981). Rheological properties of Copolyester Liquid Crystalline Melts. I. Capillary Rheometry. *Journal of Rheology*, *25*, 275-292.
- Khan, S.A., & Prud'Homme, R.K. (1987). Melt rheology of filled thermoplastics. *Reviews in Chemical Engineering*, *4*, 205-270.
- Lai, H.L., Pitt, K., & Craig, D.Q.M. (2010). Characterisation of the thermal properties of ethylcellulose using differential scanning and quasi-isothermal calorimetric approaches. *International Journal of Pharmaceutics*, *386*, 178–184.
- Lang, B., McGinity, J.W., & Williams III, R.O. (2014). Hot-melt extrusion – basic principles and pharmaceutical applications. *Drug Development and Industrial Pharmacy*, *40*, 1133-1155.
- Larson, R.G. (1999). *The Structure and Rheology of Complex Fluids*. New York: Oxford University Press.
- Laun, H.M. (1984). Orientation effects and rheology of short glass fiber-reinforced thermoplastics. *Colloid and Polymer Science*, *262*, 257-269.
- Laun, H.M. (2004). Capillary rheometry for polymer melts revised. *Rheologica Acta*, *43*, 509-528.
- Laun, H.M., & Schuch, H. (1989). Transient elongational viscosities and drawability of polymer melts. *Journal of Rheology*, *33*, 119-175.
- Macosko, C.W. (1994). *Rheology: principles, measurements and applications*. New York: Wiley-VCH Inc.; 1994.
- Maru, S.M., De Matas, M., Kelly, A., & Paradkar, A. (2011). Characterization of thermal and rheological properties of zidovudine, lamivudine and plasticizer blends with ethyl cellulose to assess their suitability for hot melt extrusion. *European Journal of Pharmaceutical Sciences*, *44(4)*, 471–478.
- Mooney, M. (1931). Explicit formulas for slip and fluidity. *Journal of Rheology*, *2*, 210-222.

- Piau, J.-M., El Kissi, N., Toussaint, F., & Mezghani, A. (1995). Distortions of polymer melt extrudates and their elimination using slippery surfaces. *Rheologica Acta*, 34, 40-57.
- Quinten, T., Gonnissen, Y., Adriaens, E., De Beer, T., Cnudde, V., Masschaele, B., Van Hoorebeke, L., Siepmann, J., Remon, J.P., & Vervaet, C. (2009). Development of injection moulded matrix tablets based on mixtures of ethylcellulose and low-substituted hydroxypropylcellulose. *European Journal of Pharmaceutical Sciences*, 37, 207–216.
- Quinten, T., De Beer, T., Almeida, A., Vlassenbroeck, J., Van Hoorebeke, L., Remon, J. P., & Vervaet, C. (2011). Development and evaluation of injection-molded sustained-release tablets containing ethylcellulose and polyethylene oxide. *Drug Development and Industrial Pharmacy*, 37, 149–159.
- Repka, M.A., Shah, S., Lu, J., Maddineni, S., Morott, J., Patwardhan, K., & Mohammed, N.N. (2012). Melt extrusion: process to product. *Expert Opinion on Drug Delivery*, 9, 105-125.
- Rosenbaum, E.E., & Hatzikiriakos, S.G. (1997). Wall slip in the capillary flow of molten polymers subject to viscous heating. *AIChE Journal*, 43, 598-608.
- Shah, S., Maddineni, S., Lu, J., & Repka, M.A. (2013). Melt extrusion with poorly soluble drugs. *International Journal of Pharmaceutics*, 453, 233-252.
- Zema, L., Loreti, G., Macchi, E., Foppoli, A., Maroni, A., & Gazzaniga, A. (2013a). Injection-molded capsular device for oral pulsatile release: development of a novel mold. *Journal of Pharmaceutical Sciences*, 102, 489–499.
- Zema, L., Loreti, G., Melocchi, A., Maroni, A., & Gazzaniga, A. (2012). Injection molding and its application to drug delivery. *Journal of Controlled Release*; 159, 324-331.
- Zema, L., Loreti, G., Melocchi, A., Maroni, A., Palugan, L., & Gazzaniga, A. (2013b). Gastroresistant capsular device prepared by injection molding. *International Journal of Pharmaceutics*, 440, 264–272.

Chapter II

The contents of this chapter have been submitted for publication:

Casati, F., Briatico-Vangosa, F., Baldi, F., Melocchi, A., Maroni, A., Gazzaniga, A., & Zema, L. (2016). Ethylcellulose-based materials for the development of prolonged-release drug delivery systems manufactured by micromolding. *Submitted*.

Ethylcellulose-based materials for the development of prolonged-release drug delivery systems manufactured by micromolding

INTRODUCTION

The exploitation of hot-processing techniques, based on the extrusion and molding of polymeric materials, is currently one of the most appealing goals of the pharmaceutical industry, especially with respect to its potential for improving the bioavailability of poorly-soluble drugs, achieving new drug delivery targets and enabling continuous manufacturing (Melocchi et al., 2015; Tiwari et al., 2016; Zema et al., 2012). Moreover, 3D printing of dosage forms, which is supporting the advent of personalized therapy, can also be performed by extrusion, as in the case of fused deposition modeling (FDM) (Genina et al., 2016; Goyanes et al., 2015; Melocchi et al., 2016; Norman et al., 2016). In this respect, injection molding (IM) and 3D printing by FDM were recently proposed for the manufacturing of new drug delivery systems (DDSs) in the form of capsular devices, which represent an advantageous alternative to traditional reservoir systems. In fact, they can be separately manufactured and filled with different types of drugs/drug formulations, governing the release performance mainly on the basis of the design and composition of the capsule shell (*e.g.* gastric resistance, delayed/pulsatile or prolonged release, colon targeting) (Gazzaniga et al., 2011; Macchi et al., 2015; Melocchi et al., 2015; Zema et al., 2013a, b). Besides thermal stability issues related to the drug substance, one of the main reasons that still limits the use of such technologies in this field is the lack of information about the thermal, rheological and stability characteristics of melts resulting from pharmaceutical formulations and of methods for the evaluation of their successful processability (Aho et al., 2015).

Ethylcellulose (EC) is a non-toxic and stable insoluble polymer that has widely been used for the production of prolonged-release dosage forms, both as monolithic devices, where the active ingredient is dispersed within the polymeric carrier, and reservoir systems, *i.e.* drug-containing cores surrounded by a release-controlling barrier, generally applied by film coating. It is well known that slowing down the release of drugs, thus sustaining their plasma concentrations over time, may be related to major improvements in the therapy efficacy and patient compliance (avoidance of multiple administrations, reduction of the overall drug dose) (Lin & Chien, 2013). Depending on the duration of release, these systems can be suitable for different sites and routes of administration. For instance, implants/inserts are able to deliver their content for days up to several months, whereas formulations intended for the oral route release their contents within 12/24 h, consistent with the gastrointestinal transit. EC has shown to be extrudable, and several monolithic DDSs manufactured by hot melt extrusion (HME) and IM were proposed based on this polymer (Bar-Shalom et al., 2003; Quinten et al., 2009, 2011). More recently, the possibility of attaining EC filaments intended for 3D printing by FDM was also demonstrated (Melocchi et al., 2016). In the present work, an investigation protocol was developed to assess the processability by micromolding (μ IM) of EC-based materials through the use of disk-shaped specimens purposely devised (screening items). The simple geometry of such a model, which has been conceived and exploited for previous rheological, mechanical and barrier performance studies of polymers of pharmaceutical interest, makes the analysis of the process and of its effects on the final product easier and faster to carry out (Melocchi et al., 2016; Treffer et al., 2015; Zema et al., 2013b). The polymeric materials under investigation would be intended for the manufacturing of insoluble barriers, such as capsule shells, coatings or matrices for prolonged-release systems, which allow biological fluids to permeate and dissolved drug molecules to diffuse

through. Demonstration of EC processability by μ IM and its in-depth understanding may also promote development of new DDSs manufactured by this technique, either intended for oral or non-oral administration routes.

MATERIALS AND METHODS

Materials

Ethylcellulose, EC (EthocelTM Std. 100 FP premium; Dow, US): particle size $\leq 150 \mu\text{m}$, mean particle size 30-60 μm ; ethoxyl content 48.0-49.5 %wt; the viscosity of 5% solution in 80% toluene and 20% alcohol (25 °C; Ubbelohde viscometer) 90-110 mPa·s; molecular weight not provided by the producer. Triethyl citrate, TEC (Aldrich, Germany). Polyvinyl alcohol-polyethylene glycol graft copolymer, KIR (Kollicoat[®] IR; BASF, Germany): MW $\approx 45.000 \text{ Da}$; $d_{50} = 23 \mu\text{m}$ and $d_{90} = 55 \mu\text{m}$. Low-substituted hydroxypropylcellulose, LHPC (L-HPC NBD 020; Shin-Etsu, Japan): $d_{50} = 42.6 \mu\text{m}$ and $d_{90} = 91.1 \mu\text{m}$; hydroxypropoxy content 14%. Blue dye-containing preparation (Kollicoat[®] IR Brilliant Blue, BASF, Germany), acetaminophen (Rhodia, Italy).

Methods

Preparation of materials

Plasticized EC- Plasticized EC mixtures (ECTEC) containing 10, 20 and 25% by weight (%wt) of TEC (ECTEC10, ECTEC20 and ECTEC25, respectively), calculated on the dry polymer, were prepared by kneading (Baldi et al., 2016). EC powder was placed in a mortar and the liquid plasticizer was added dropwise under continuous mixing. The resulting blend was left 12 h at room conditions ($21 \pm 5 \text{ °C}$, $55 \pm 5\% \text{ RH}$). Afterwards, aggregates were ground by means of a blade mill and the $< 250 \mu\text{m}$ fraction was recovered.

Plasticized blends- Blends of milled ECTEC20 with a release modifier powder, KIR or LHPC, in a 7:3 (30KIR and 30LHPC), 5:5 (50KIR) and 4:6 (60KIR) weight ratio were prepared. KIR and LHPC powders were previously dried in an oven (40 °C for 24 h). ECTEC20 and the release modifier were mixed in a mortar for less than 1 minute; physical mixtures were stored in plastic bags under vacuum and used within one or two days.

Rheological studies

The flow behavior of neat and plasticized EC was evaluated by resorting to the slit capillary die (width 10 mm, height 1.5 mm, length 75 mm) integrated in the recirculation channel of Haake™ MiniLab II (Thermo Scientific™, US) microcompounder, equipped with two conical screws (diameter 5/14 mm, length 109.5 mm) in counter-rotating configuration. Samples of 10 g were manually fed into the microcompounder. Data were collected at 165 °C and 175 °C. At each extrusion temperature, a series of measurements was carried out at screw rotation speeds from 10 to 200 rpm, acquiring data at 15 logarithmically spaced points. For each speed, the difference in pressure between the exit and the entrance of the channel, ΔP , was monitored and recorded when a stable constant value was reached. The ΔP values vs revolution speed were then processed according to Yousfi et al. (2014) in order to obtain apparent viscosity curves. In Figure 1 the results obtained by this procedure applied to ECTEC20 are compared with those from standard capillary viscosimetry tests performed on the same material (Baldi et al., 2016). Even if the overlapping of apparent shear rate ranges investigated by the two techniques is limited to one point, the overall trend seems to confirm the reliability of the measurements performed in this work.

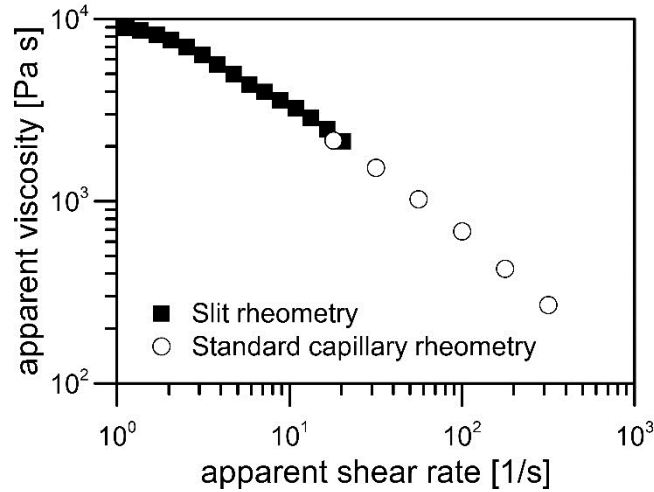


Figure 1. apparent viscosity vs shear rate curves at 175 °C for ECTEC20, measured through capillary rheometry (adapted from Baldi et al., 2016) and slit rheometry in the Haake™ MiniLab II microcompounder.

Moldability studies

Micromolding (μ IM) trials were carried out by a bench-top hydraulic press (BabyPlast 6/10P; Cronoplast S.L., S; Rambaldi S.r.l., Italy), equipped with a 10 mm piston and cooling circuit. 50 g samples were loaded into the μ IM press hopper and extruded from the injecting unit as during a purge operation (air shot test) (Rosato et al., 2000); the test was repeated under different operating temperatures.

Short shot test

ECTEC materials were processed by the μ IM press equipped with a disk-shaped mold (diameter 30 mm) provided with a central gate and allowing to set different values of cavity thickness, *i.e.* 1000, 600, 400 and 200 μ m. The molding process is pressure-controlled and based on two stages: the first-stage pressure (P_1) supports the filling of the mold cavity, while the second-stage one (P_2) leads to proper packing of the material until it solidifies (Rosato et al., 2000). During short shot tests, the influence of the filling step on

the melt progression throughout the mold was only considered, while P_2 was kept constant at the lowest setting conditions (Table 1).

Table 1. μ M conditions for the manufacturing of screening disks based on ECTEC materials.

Process parameter		value
compression zone temperature; °C		170
metering zone temperature; °C		175
nozzle temperature; °C		175
1 st injection	pressure; <i>bar</i>	varied from 10 to 100
	time; <i>s</i>	varied from 1.0 to 2.5
2 nd injection	pressure; <i>bar</i>	10
	time; <i>s</i>	0.0
cooling time; <i>s</i>		2.5

Several injection tests at different P_1 values (10-100 bar, 10 bar increments) and fill time of 1.0 s were initially performed. When incomplete disks were obtained, the fill time was increased up to 2.5 s (0.5 s increments), while keeping all the other settings constant.

Digital photographs of disks, both complete and incomplete, were taken (Nikon D70, Nikon, Japan) and analyzed by ImageJ. As the image processing software requires a sharp contrast between the scanned object and the background, transparent EC-based disks were coated with a white acrylic paint and laid on a black background. Aspect ratio (AR) (eq. 1) and effective radius (R_{eff}) (eq. 2) of disks were calculated using the major axis (R_{max}) and minor axis (R_{min}) of the best fitting ellipses:

$$AR = R_{\text{max}}/R_{\text{min}} \quad (\text{eq. 1})$$

$$R_{\text{eff}} = (R_{\text{max}} + R_{\text{min}})/2 \quad (\text{eq. 2})$$

Evaluation of molded products

Dimensional stability

To investigate the tendency to shrinkage and warpage of the molded products, 400 μm screening disks were molded at P_1 values of 40 (ECTEC10) or 30 (ECTEC20 and ECTEC25) bar and a fixed fill time of 1 s, followed by a 1 s packing phase carried out at such P_2 values that the difference between packing and filling pressures, $\Delta P (= P_2 - P_1)$, turned out equal to -20, 0, 30 and 60 bar. Images of the disks were taken by a digital camera (Nikon D70, Nikon, Japan) immediately after molding and after storage at ambient conditions ($t = 1 \text{ h}, 24 \text{ h}, 48 \text{ h}, 72 \text{ h}$ and 10 days) or exposure to a 15 min thermal treatment inside the heating chamber of a thermal balance (Mettler PM100 equipped with Mettler LP 15, Mettler-Toledo, Italy) at 40, 50, 60, 70, 80 and 120 $^{\circ}\text{C}$. A deformation score, based on an arbitrarily defined scale (ranging from 0 to 5), was attributed comparing samples of the same composition maintained under different storage conditions.

Barrier performance

600 μm thick disks were evaluated in terms of water uptake, mass loss and permeability to aqueous fluids. When ECTEC blends with release modifiers were employed, the influence of the method of preparation (mixing efficiency) on the characteristics of the molded barriers was first considered. The blends obtained as described in *Preparation of materials* were extruded by a single-screw extruder (Extrusiograph 19/25D, Brabender, Germany) equipped with a 4 mm rod-shaped die (processing temperatures in the 125-140 $^{\circ}\text{C}$ range and rotational speed 15 rpm). 50 g samples of pellets obtained by manually cutting the extruded rods were then used to fill the μIM press. ECTEC materials of analogous composition as obtained from air shot tests showed similar aspect and comparable resistance to manual rupture immediately after ejection and after cooling, independent of

the method by which the material was obtained. Moreover, few disks based on the 30KIR and 30LHPC formulations were prepared starting from both physical mixture and extruded pellets. As after processing under the same conditions, the mixture and the pellets led to disks that showed comparable physical characteristics and permeability behavior, the preparation of ECTEC materials by mixing of powders was preferred for simplicity.

Water uptake and mass loss test

The mass loss test was carried out by adapting a method described in the literature to the shape and dimensions of samples (Karrout et al., 2009). Cylindrical samples (diameter 11 mm; n = 3), die cut from molded disks dried in an oven at 40 °C (24 h), were hung up on a purposely-designed support through a hole that was manually punched on each of them by means of a needle of 0.8 mm in diameter. The support was immersed in 125 mL of distilled water at 37 ± 0.5 °C stirred at 120 rpm (magnetic stirrer). At pre-determined times t_x , x = 1 h, 2 h, 4 h, 8 h and 24 h, samples were withdrawn, blotted and weighed (wet mass). After this procedure, they were dried in an oven at 40 °C for 24 h and weighed (dry mass). Water uptake (WU) and dry mass loss (DML) were calculated according to equations 3 and 4, respectively.

$$\text{WU}\% (t_x) = (\text{wet mass, } t_x - \text{dry mass, } t_x / \text{wet mass, } t_x) * 100 \quad (\text{eq. 3})$$

$$\text{DML}\% (t_x) = (\text{dry mass, } t_0 - \text{dry mass, } t_x / \text{dry mass, } t_x) * 100 \quad (\text{eq. 4})$$

Permeability test

Permeability tests were carried out with EC disks employing manually-assembled cells (area exposed to the medium = 177 mm²) modified from the extraction cells used for the dissolution test for transdermal patches (2.9.4 Dissolution test for transdermal patches - Cell method, Ph. Eur. 9.1) (Melocchi et al., 2016; Zema et al., 2013b). Molded disks were

mounted to close the cell cavity, which was filled with approximately 50 mg of acetaminophen powder or a blue dye-containing preparation as the tracer (Figure 2). The test ($n = 3$) was performed by a USP 38 dissolution apparatus 2 (Dissolution System 2100B, Distek, US) in 500 mL of distilled water at 37 ± 0.5 °C, paddle rotating speed 100 rpm.

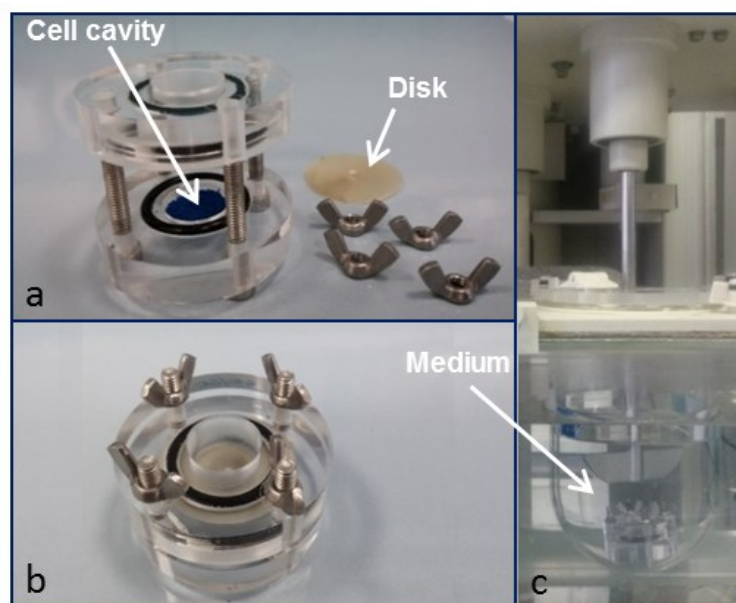


Figure 2. Cell for the evaluation of molded disk permeability: (a) partially assembled, with the cell cavity filled with a dye tracer; (b) assembled for the test and (c) positioned into a vessel of the dissolution apparatus.

When cells were loaded with the drug tracer, fluid samples were withdrawn from dissolution vessels at fixed time points over 24 h and assayed spectrophotometrically at 244 nm (spectrophotometer Lambda25, Perkin Elmer, US). Cells filled with the dye-containing formulation were visually inspected over 30 days. By employing a dye tracer, the time taken by the solvent to permeate the polymeric barrier was assessed through the

blue coloring inside the cell cavity. At the end of the test, disks were collected from the cells and photographed.

Scanning Electron Microscopy, SEM

SEM analysis of disks was carried out before and after immersion in water at 37 °C, under magnetic stirring, for 7 days, followed by drying in a ventilated oven at 40 °C for 24 h. The disks were then broken under liquid nitrogen, in such a way as to obtain a fracture surface almost perpendicular to the direction of the material flow during mold filling, and the cryo-fractured surface was studied by SEM (model Zeiss Evo 50 EP, Germany) operating in high vacuum mode. The surface, prior to be analyzed, was sputtered with a thin layer of gold.

RESULTS AND DISCUSSION

Evaluation of the material processability

Rheological studies

A rheological characterization of materials under a compounding step was preliminarily performed, in order to assess the effect of plasticizer content and select the temperature conditions for the μ IM trials. The need for a plasticizer (TEC) to enable processing of EC below its decomposition temperature (≈ 180 °C), *i.e.* in the 170-175 °C range, was already demonstrated by capillary rheometry studies (Baldi et al., 2016). In particular, it was shown that the addition of 20 %wt TEC lowers the viscosity at any fixed shear rate and, more interestingly, gives to the viscosity curve a pronounced shear thinning characteristic. Results of this characterization confirmed such findings at all the considered plasticizer contents, as shown in Figure 3. In addition, the temperature increase was shown to significantly lower the apparent viscosity.

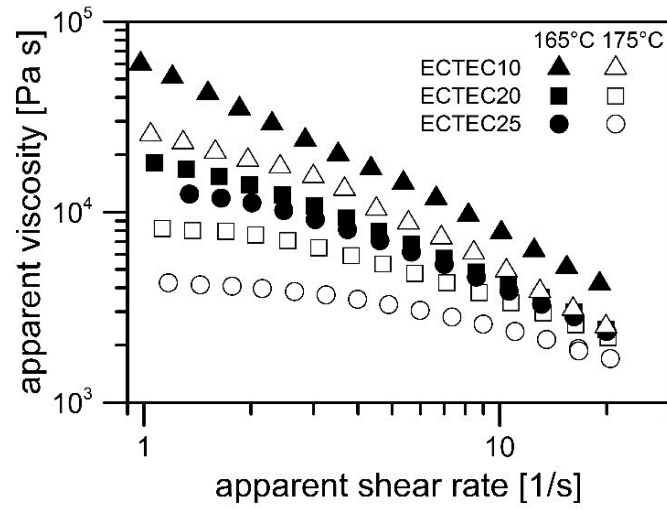


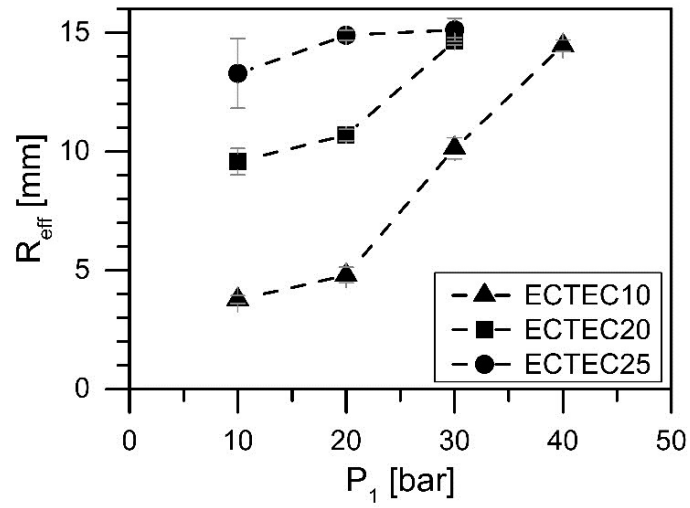
Figure 3. Apparent viscosity vs apparent shear rate of EC TEC mixtures as a function of temperature and TEC content.

The effect of plasticizer content was more evident at high temperature and low apparent shear rates, while the effects of both temperature and TEC content tended to decrease at high shear rates. It can thus be assumed that under μ IM processing, where shear rates are expected to be higher, also above the maximum value explored in the slit capillary die rheometer, differences in the behavior of the various formulations would relatively be limited. However, during injection into the disk-shaped mold, the flow of the material was neither isothermal nor stationary, as in the rheometer. Thus, rheological data may only give rough information about the behavior of materials under real processing. In order to more in-depth investigate this aspect, a series of molding experiments were performed.

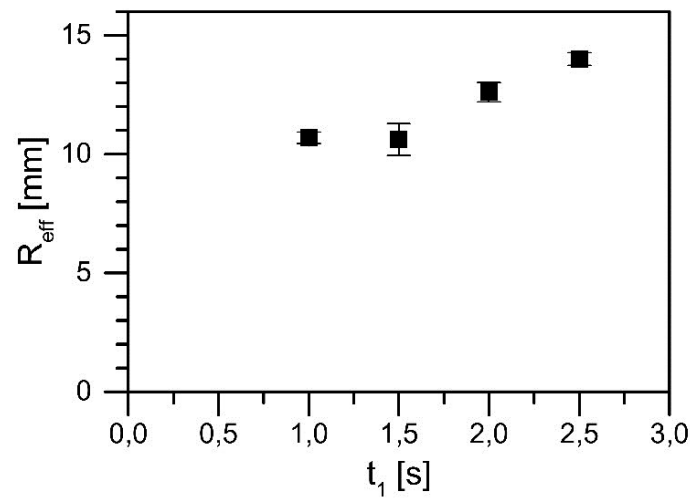
Moldability studies

An investigation protocol based on the evaluation of short shots was developed to assess the effect of TEC on EC moldability and determine appropriate molding conditions of ECTEC mixtures. From preliminary tests, the mold cavity that could completely be filled to give the thinnest disks turned out to be the 400 μm thick one. Using this mold cavity, a wide range of filling conditions was investigated, including the injection pressure (10-100 bar), fill time (1-2.5 s) and plasticizer amount (10-25 %wt). All the other process parameters were kept constant (see Table 1 in Methods section *Short shot test*).

In all experiments, irrespective of whether the mold cavity was partly or completely filled, the aspect ratio (AR) of resulting disks, either complete or incomplete, turned out very close to 1. Thus, the base of screening specimens was circular and the measured radius (R_{eff}) was observed to increase up to 15 mm, *i.e.* the nominal radius of a complete disk, by raising the injection pressure (setting fill time at 1 s) (Figure 4a). The ECTEC material containing the lowest amount of plasticizer, and therefore characterized by the highest viscosity at each shear rate, required the greatest pressure to completely fill the mold, while almost complete disks were obtained with ECTEC25 already at the lowest P_1 value. The effect of fill time at a pressure of 20 bar was also investigated. Figure 4b, shows that, with ECTEC20, complete cavity filling could be attained provided that enough time was allowed. However, this was not observed with all the formulations and process conditions. Indeed, during other tests performed at lower pressure values, complete filling was never achieved, even in a longer time, due to the early freezing of the material inside the mold.



a



b

Figure 4. Effective radius (R_{eff}) of (a) disks with different TEC content produced at increasing injection pressure (P_1) and fixed fill time of 1.0 s, (b) ECTEC20 disks produced at increasing fill time (t_1) and fixed P_1 of 20 bar. $n = 6$; bars in figures represent standard deviation.

Dimensional stability

The tendency of disks to shrinkage and warpage was evaluated, in order to finally select the most adequate material composition and process parameters for the relevant production. Starting from the minimum P_1 value required to have the mold cavity completely filled with each ECTEC mixture (see Fig. 4a), a set of disks were molded at increasing $\Delta P (= P_2 - P_1)$ levels, from -20 to 60 bar. The deformation of such items stored at ambient conditions and after exposure to high temperatures (up to 120 °C) was investigated over time (10 days after demolding). No deformation was shown by disks stored at room temperature, regardless of the amount of plasticizer and of pressures applied during the molding process. In the case of samples exposed to heating treatments, changes in shape (bending and twisting) and diameter (reduction) were observed, which turned out dependent on the amount of plasticizer in the polymeric mixture, on the temperature and on the ΔP applied. Figure 5 reports both the minimum temperature at which warpage was observed and the extent of deformation of disks maintained for 15 min at the highest temperature of 120 °C, as a function of TEC content and process pressures.

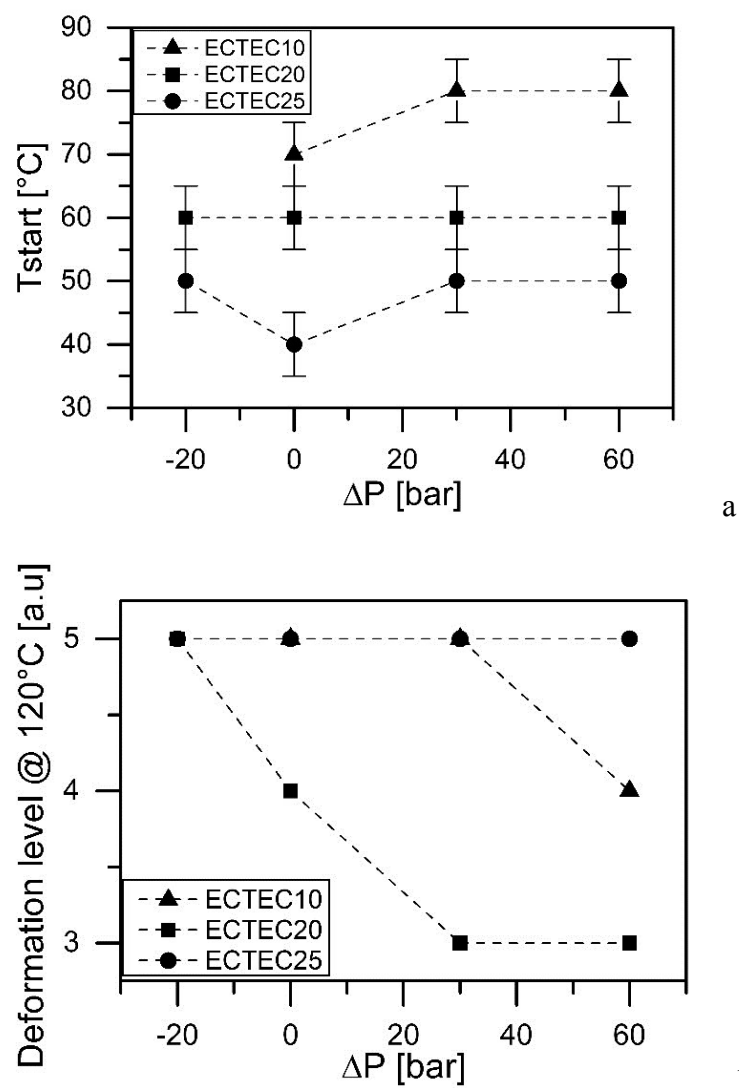


Figure 5. Curves of (a) minimum temperature of warpage (T_{start}) and (b) extent of deformation after a 120 °C treatment of disks vs ΔP (= $P_2 - P_1$) applied during the molding process as a function of TEC content in the material.

The minimum temperature after exposure to which disks showed warpage seemed almost independent of the pressures applied during the molding process, whereas it decreased with the increase of plasticizer content in the material. This can be explained by the increase in molecular mobility (at a given temperature) promoted by TEC, which is reflected in the reduction of the glass transition temperature of EC/TEC mixtures at increasing TEC content, from 127 °C for neat EC to 80, 60 and 45 °C for ECTEC10, ECTEC20 and

ECTEC25, respectively. Glass transition temperature (T_g) was estimated by Dynamical Mechanical Analysis, carrying out heating ramps at the rate of 10 °C/min; T_g was defined as the temperature at which the conservative component of complex modulus, E' , starts decreasing. As for maximum deformation at 120 °C, the expected beneficial effect of applying a packing pressure was observed only in the case of disks made of ECTEC20 and, to a lower extent, of ECTEC10.

Therefore, the overall results indicated that 20 %wt of plasticizer would offer the best balance of molding ability of the ECTEC mixture and dimensional stability of the molded object, also taking possible changes in the composition of the material into account. In fact, while the addition of charges, potentially useful to improve the permeability of the polymeric barrier thus increasing the release performance, should enhance the dimensional stability, the presence of polyvinyl alcohol-polyethylene glycol graft copolymer (KIR) and low-substituted hydroxypropyl cellulose (LHPC) particles was already shown to be responsible for an increase in the melt viscosity without affecting the shear-thinning behavior of the material (Baldi et al., 2016).

Evaluation of molded material performance

Molded disks could advantageously be exploited for assessing the potential of materials under development as components of polymeric barriers intended for controlling the release rate of active ingredients from reservoir delivery systems. In particular, the ability to take up water, the mass loss resulting from dissolution of soluble components and erosion phenomena as well as the rate of diffusion of tracers through the molded barrier were investigated. The addition to the ECTEC formulation of solid (charges) KIR and LHPC, a soluble and an insoluble additive, respectively, which may act as release modifiers by modulating the permeability of the molded barrier, was also considered

(Häbel et al., 2016). The channeling action of such additives in molded barriers was already demonstrated and attributed to particle dissolution in the case of KIR, and formation of tears as a consequence of swelling in that of LHPC (Zema et al., 2013a).

Disks based on the selected ECTEC20 formulation and containing increasing amounts of the solid additives were prepared. KIR and LHPC confirmed the tendency to increase the viscosity of melts, as dynamically measured by rotational rheometry (Baldi et al., 2016). Therefore, a mold cavity having thickness of 600 μm , which was deemed less challenging than 400 μm , was employed, and process parameters were accordingly adjusted (Table 2). In particular, the shot size was increased and the injection pressure was decreased. Due to some limitations in the processability of EC-based dispersions, the influence of the amount of release modifier added to ECTEC20 was investigated up to 60 %wt only with those containing KIR. The increase in the number of solid particles in the melt, in fact, involved the use of higher pressures and pointed out some criticalities in the mechanical resistance of disks during automatic ejection.

Table 2. μIM conditions for the manufacturing of 600 μm thick disks containing different type and amount of release modifiers.

Process parameter	Polymeric formulation				
	ECTEC20	30LHPC	30KIR	50KIR	60KIR
compression zone temperature; $^{\circ}\text{C}$	170			170	180
metering zone temperature; $^{\circ}\text{C}$	175			175	185
nozzle temperature; $^{\circ}\text{C}$	175			175	185
1 st injection pressure; <i>bar</i>	20			30	30
injection time; <i>s</i>	1.0			2.0	2.0
2 nd injection pressure; <i>bar</i>	80			90	90
injection time; <i>s</i>	1.0			1.0	1.0
cooling time; <i>s</i>	2.5			2.5	10

Water uptake (WU) and dry mass loss (DML) profiles over 24 h relevant to molded disks containing different type and amount of release modifiers are shown in Figure 6.

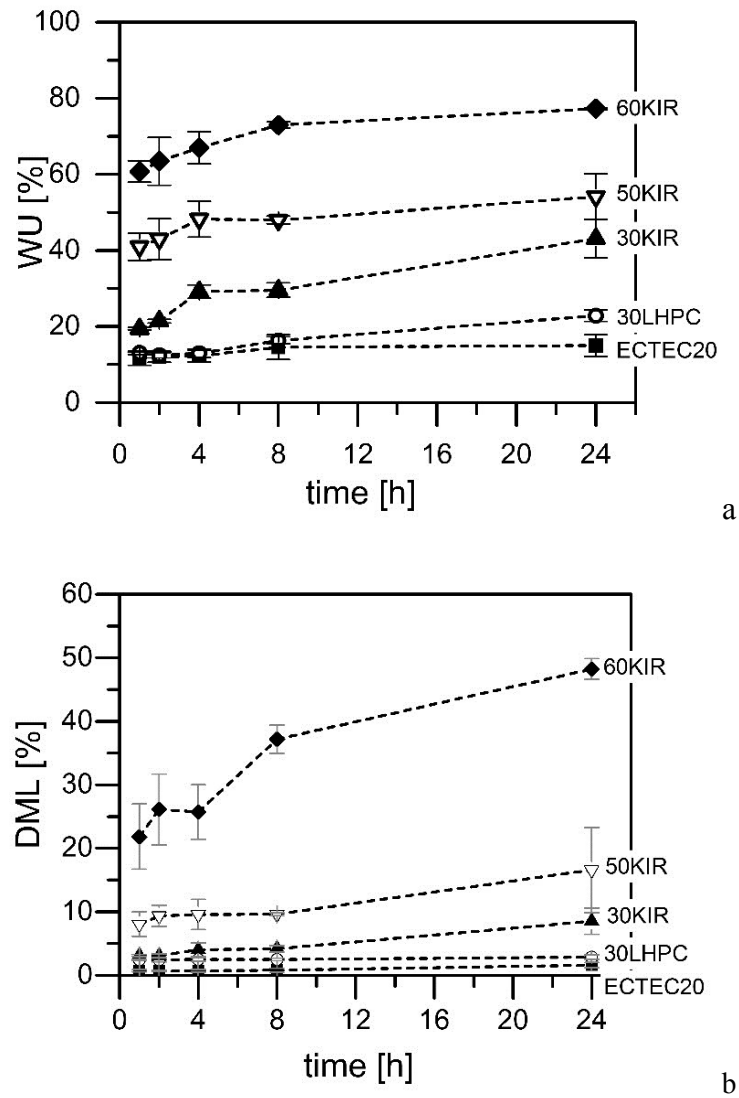


Figure 6. (a) WU and (b) DML profiles of molded disks based on ECTEC20 containing different type and amount of release modifiers.

In all cases, the highest rate of WU was observed at the beginning of the test and turned out to be strongly influenced by the composition of EC-based dispersions. Indeed, the water content of samples after 1 h increased from about 12% in the case of ECTEC20 to 60% of the disks with maximum KIR load (60KIR). During the next several hours, water

uptake tended to slow down considerably: water content of disks never increased more than 10% from 8 to 24 hours. The ability of materials with the same load of adjuvant to take up water was higher when soluble KIR was used as the release modifier. As regards mass loss, the highest rate was observed for all samples in the first hour of the test. The values reached, generally maintained over 24 h, tended to slightly decrease with increasing amounts of KIR in the material. This suggests that the mass loss of molded disks should be attributed to the release of soluble components. Although very limited, the mass loss of ECTEC20 disks was probably due to the leaching of the plasticizer. Indeed, TEC is known to have < 10% miscibility with water (Snejdrova & Dittrich, 2012). DML profiles of disks containing the insoluble release modifier LHPC were almost superimposed to those relevant to disks without any adjuvant (ECTEC20), ruling out a major impact of the polymer swelling on the molded barrier integrity. The mass loss after 24 h in aqueous fluids did not even exceed 20% in samples containing 50% of release modifier; only with 60KIR the initial weight of disks was nearly halved. In all cases, polymeric barriers showed practically unchanged dimensions and surface aspect after 24 h test.

SEM photomicrographs of ECTEC20 disks containing 30 %wt of KIR, analyzed before and after being in contact with distilled water for 7 days (followed by drying), seem to confirm the hypothesis that KIR leach out of the disk barrier by dissolving in the aqueous fluid (Figure 7). As a matter of fact, KIR particles can clearly be observed in the “as produced” sample (Fig. 7a), while no inclusion having the same aspect can be identified in the sample after immersion in water (Fig. 7b). In the latter sample, isolated voids can be distinguished that do not appear interconnected to form a network, which may represent a critical issue in molded systems intended for drug release, as already highlighted with scaffolds (Kramschuster & Turng, 2010; Mi et al., 2014).

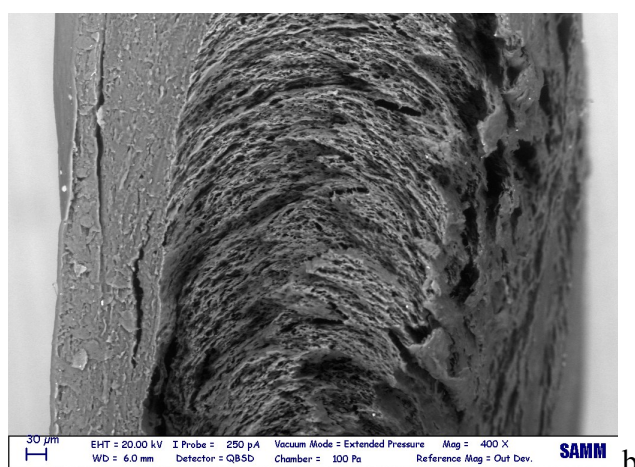
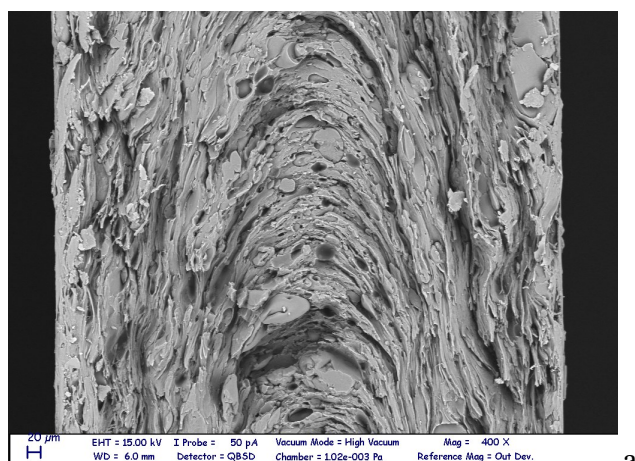
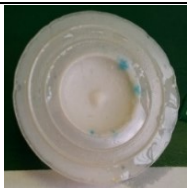

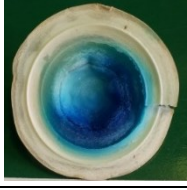
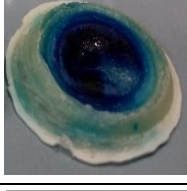
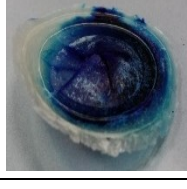


Figure 7. SEM photomicrographs of the cross section of 600 μm thick ECTEC20 disks containing 30 %wt of KIR (a) immediately after molding and (b) after immersion in stirred water for 7 days.

Finally, the barrier performance of molded disks was studied by positioning them to close the cavity of permeability cells filled with a acetaminophen as a tracer and immersed in stirred distilled water (dissolution apparatus). Acetaminophen was not detected in the medium after 24 h, independent of the composition of the molded barrier. Therefore, a longer screening test (30 days) using a dye tracer was carried out, and the results are collected in Table 3. The appearance of an intense blue coloration inside the cell cavity was used to define the time for the solvent front to permeate the polymeric barrier. On the other hand, coloration of the medium, which would indicate the lag time before permeation

of the dye across the barrier, was more difficult to visually be detected because of dilution. Moreover, the morphological characteristics of molded disks withdrawn from the cells after 30 days were evaluated.

Table 3. Data relevant to permeability tests of 600 μm thick disks.

Polymeric formulation	Appearance of blue color inside the cell cavity	Aspect of disks after 30 days		
		Color intensity	Integrity	
ECTEC20	no	-	yes	
30LHPC	no	-/+	yes	
30KIR	no	+	yes	
50KIR	after 8 days	++	yes	
60KIR	after 3-5 days	++	no (evidence of cracks)	

ECTEC20 disks were confirmed to be very slowly permeable to aqueous fluids. In fact, after 30 days, no coloration was observed inside the cell cavities yet. Moreover, the cavity-exposed face of the disks withdrawn appeared practically uncolored and the powder loaded

into the cell was found dry. The presence of release modifiers in the polymeric barrier generally improved the solvent penetration rate, more markedly in the case of KIR as a function of the relevant amount. The time for solvent permeation, highlighted by blue coloration inside the cell cavity, was reduced to 5 days. However, disks containing 60% of KIR, when withdrawn from the cell after 30 days of testing, showed some little cracks on the surface suggesting a possible threshold of particle load that may still be compatible with maintenance of the barrier resistance. These results are in good agreement with the hypothesized effect of LHPC and KIR as release modifiers. The permeability characteristics of the EC barriers obtained could be consistent with the performance of implantable systems with very slow release kinetics. However, different strategies to improve the rate of diffusion across the polymer barrier should be identified in order to exploit EC-based materials for the manufacturing by μ IM of capsular devices intended for the oral route.

CONCLUSIONS

In the present work, an investigation protocol for the evaluation of the processability of pharmaceutical-grade polymers by μ IM was developed, involving rheological studies of material candidates and manufacturing as well as characterization of molded screening specimens. The protocol turned out useful for assessing the effect of the type and amount of plasticizer on the moldability of EC, an insoluble polymer largely employed for the formulation of prolonged-release drug delivery systems.

The use of disk-shaped specimens allowed meaningful data to be collected about IM processability of EC-based materials. Moreover, when used as drug diffusion barriers, they helped highlight technological and performance features of molded structures composed of

such materials. Since permeation of aqueous fluids through these molded barriers was found very slow, the addition of permeability modifiers was also explored and successfully accomplished, in spite of some limitations encountered when processing the EC-based dispersions. Interesting results were obtained in terms of improved drug permeation rate across EC barriers, although these still failed to be consistent with oral delivery applications. Future studies will thus be required for the evaluation of new release modifiers (charges) that may promote the formation of an interconnected pore structure acting as a continuous path for drug diffusion, thus allowing release rates suitable for orally-administered systems such as capsular devices to be attained.

REFERENCES

- Baldi, F., Ragnoli, J., Zinesi, D., Bignotti, F., Briatico-Vangosa, F., Casati, F., Loreti, G., Melocchi, A. & Zema, L. (2016). Rheological characterization of ethylcellulose-based melts for pharmaceutical applications. *AAPS PharmSciTech*. <http://doi.org/10.1208/s12249-016-0577-0>.
- Bar-Shalom, D., Slot, L., Wang Lee, W., & Wilson, C. G. (2003). Development of the Egalet® technology. In Rathbone, M. J., Hadgraft, J., & Roberts, M. S. (Eds.), *Modified-release drug delivery technology* (pp. 263–271). New York: Marcel Dekker.
- Gazzaniga, A., Cerea, M., Cozzi, A., Foppoli, A., Maroni, A., & Zema, L. (2011). A novel injection-molded capsular device for oral pulsatile delivery based on swellable/erodible polymers. *AAPS PharmSciTech*, *12*, 295–303.
- Genina, N., Holländer, J., Jukarainen, H., Mäkilä, E., Salonen, J., & Sandler, N. (2016). Ethylene vinyl acetate (EVA) as a new drug carrier for 3D printed medical drug delivery devices. *European Journal of Pharmaceutical Sciences*, *90*, 53–63.
- Goyanes, A., Wang, J., Buanz, A., Martínez-Pacheco, R., Telford, R., Gaisford, S., & Basit, A. W. (2015). 3D Printing of Medicines: Engineering Novel Oral Devices with Unique Design and Drug Release Characteristics. *Molecular Pharmaceutics*, *12*, 4077–4084.
- Häbel, H., Andersson, H., Olsson, A., Olsson, E., Larsson, A., & Särkkä, A. (2016). Characterization of pore structure of polymer blended films used for controlled drug release. *Journal of Controlled Release*, *222*, 151–158.
- Karrout, Y., Neut, C., Wils, D., Siepmann, F., Deremaux, P., Desreumaux, P., & Siepmann, J. (2009). Novel polymeric film coatings for colon targeting: How to adjust desired membrane properties. *International Journal of Pharmaceutics*, *371*, 64–70.
- Kramschuster, A., & Turng, L.-S. (2010). An injection molding process for manufacturing highly porous and interconnected biodegradable polymer matrices for use as tissue engineering scaffolds. *Journal of Biomedical Materials Research. Part B: Applied Biomaterials*, *92*, 366–376.
- Lin, S., & Chien, Y. W. (2013). Drug Delivery: Controlled Release. In *Encyclopedia of Pharmaceutical Science and Technology* Fourth Edition (pp. 955–984). New York: Taylor and Francis.

- Macchi, E., Zema, L., Maroni, A., Gazzaniga, A., & Felton, L. A. (2015). Enteric-coating of pulsatile-release HPC capsules prepared by injection molding. *European Journal of Pharmaceutical Sciences*, *70*, 1–11.
- Melocchi, A., Loreti, G., Del Curto, M. D., Maroni, A., Gazzaniga, A., & Zema, L. (2015). Evaluation of hot melt extrusion and injection molding for continuous manufacturing of immediate release tablets. *Journal of Pharmaceutical Sciences*, *104*, 1971–1980.
- Melocchi, A., Parietti, F., Maroni, A., Foppoli, A., Gazzaniga, A., & Zema, L. (2016). Hot-melt extruded filaments based on pharmaceutical grade polymers for 3D printing by fused deposition modeling. *International Journal of Pharmaceutics*, *509*, 255–263.
- Mi, H.-Y., Jing, X., Salick, M. R., Turng, L.-S., & Peng, X.-F. (2014). Fabrication of thermoplastic polyurethane tissue engineering scaffold by combining microcellular injection molding and particle leaching. *Journal of Materials Research*, *29*, 911–922.
- Norman, J., Madurawe, R. D., Moore, C. M. V., Khan, M. A., & Khairuzzaman, A. (2016). A new chapter in pharmaceutical manufacturing: 3D-printed drug products. *Advanced Drug Delivery Reviews*. <http://dx.doi.org/10.1016/j.addr.2016.03.001>
- Quinten, T., Gonnissen, Y., Adriaens, E., De Beer, T., Cnudde, V., Masschaele, B., Van Hoorebeke, L., Siepmann, J., Remon, J.P., & Vervaet, C. (2009). Development of injection moulded matrix tablets based on mixtures of ethylcellulose and low-substituted hydroxypropylcellulose. *European Journal of Pharmaceutical Sciences*, *37*, 207–216.
- Quinten, T., De Beer, T., Almeida, A., Vlassenbroeck, J., Van Hoorebeke, L., Remon, J. P., & Vervaet, C. (2011). Development and evaluation of injection-molded sustained-release tablets containing ethylcellulose and polyethylene oxide. *Drug Development and Industrial Pharmacy*, *37*, 149–159.
- Rosato, D. V., Rosato, D. V., & Rosato, M. G. (2000). *Injection Molding Handbook*. Springer Science & Business Media, 3rd Ed. Massachusetts: Kluwer Academic Publishers.
- Snejdrova, E., & Dittrich, M. (2012). Pharmaceutically used plasticizers. In Mohammad Luqman (Ed.), *Recent advances in plasticizers* (pp. 45–68). Rijeka, Croatia: InTech.
- Tiwari, R. V., Patil, H., & Repka, M. A. (2016). Contribution of hot-melt extrusion technology to advance drug delivery in the 21st century. *Expert Opinion on Drug Delivery*, *13*, 451–464.

- Treffer, D., Troiss, A., & Khinast, J. (2015). A novel tool to standardize rheology testing of molten polymers for pharmaceutical applications. *International Journal of Pharmaceutics*, *495*, 474–481.
- Yousfi, M., Alix, S., Lebeau, M., Soulestin, J., Lacrampe, M.-F., & Krawczak, P. (2014). Evaluation of rheological properties of non-Newtonian fluids in micro rheology compounder: Experimental procedures for a reliable polymer melt viscosity measurement. *Polymer Testing*, *40*, 207–217.
- Zema, L., Loreti, G., Macchi, E., Foppoli, A., Maroni, A., & Gazzaniga, A. (2013a). Injection-molded capsular device for oral pulsatile release: development of a novel mold. *Journal of Pharmaceutical Sciences*, *102*, 489–499.
- Zema, L., Loreti, G., Melocchi, A., Maroni, A., & Gazzaniga, A. (2012). Injection Molding and its application to drug delivery. *Journal of Controlled Release*, *159*, 324–331.
- Zema, L., Loreti, G., Melocchi, A., Maroni, A., Palugan, L., & Gazzaniga, A. (2013b). Gastroresistant capsular device prepared by injection molding. *International Journal of Pharmaceutics*, *440*, 264–272.

Chapter III

The contents of this chapter belong to a draft to be submitted for publication:

Casati, F., Karrout, Y., Siepmann, F., Siepmann, J., Zema, L., & Gazzaniga, A. (2016) Micromolded capsular containers for colon targeting based on the combination of time-controlled and enzyme-triggered approaches. *Draft to be submitted for publication.*

Micromolded capsular containers for colon targeting based on the combination of time-controlled and enzyme-triggered approaches

INTRODUCTION

In the field of modified-release of drugs, during recent years great efforts have been made in order to develop drug delivery systems (DDSs) able to release the conveyed drug in specific regions of the gastrointestinal tract (GIT) after oral administration. In particular, attention for the colon targeting of drugs has been pursued (Amidon et al., 2015; Maroni et al., 2010, 2013; Van Den Mooter 2006). Site-specific release in the colonic region allows the local treatment of specific diseases, such as inflammatory bowel disease (IBD), or the prevention of colorectal adenocarcinoma (Gazzaniga et al., 2006), and promotes the oral bioavailability of peptides and proteins drugs (Bourgeois et al., 2005; Sinha et al., 2007).

In order to convey drugs into the colonic region various design strategies have been pursued, especially based on reservoir systems. They refer to two main approaches: the chemical-microbiological approach and the technological-physiological one. All these strategies exploit changing physiological characteristics of the GIT when moving to the colonic region (Maroni et al., 2013). However, all the strategies are characterized by some limitations due to the high inter- and intra-variability of the GIT environment, especially in pathological conditions.

Among the colon-specific drug delivery systems, the microbially and/or enzymatically driven ones, consisting of biodegradable polymers (*e.g.*, polysaccharides) or prodrugs, are of particular interest; both are intended to be *in situ* degraded or activated, respectively, through reactions that take place selectively in the colon (Patel & Amin, 2011). Furthermore, in support of this approach, recent *in vivo* studies in healthy volunteers have

shown that bacterially-triggered drug delivery systems seem to be more reliable and reproducible than pH-triggered devices (McConnell et al., 2008). Many polysaccharides have been investigated for their potential to be selectively degraded in the colon, such as pectin (Liu et al., 2003; Tung et al., 2016; Wong et al., 2011), guar gum (Prasad et al., 1998; Seeli & Prabakaran, 2016) and chitosan (Cerchiara et al., 2016; Harding, 2016). In addition, also starch derivatives, especially resistant starch, modified to be selectively degraded in the colonic environment, have been proposed (Cummings et al., 1996a; Englyst et al., 1996; Freire et al., 2009; Karrout et al., 2009a, 2009b, 2015). High-amylose maize starch, in particular, which demonstrated resistance to pancreatic alpha-amylase and sensitivity to degradation by colonic bacterial enzyme, has been widely used (Macfarlane & Englyst, 1986; Ring et al., 1988).

The time-dependent approach to colon targeting exploits the relative reproducibility of the transit throughout the small intestine, reported to take 3 h (\pm 1 h SE), in spite of differing size and density characteristics of the dosage form and feeding state of subjects (Davis 1985; Davis et al., 1986). Therefore, formulations designed for a timely onset of the bioactive molecule release, through either coating layers or capsule plugs with inherent delaying ability, have been used to yield colon targeting after a programmed lag phase aimed at covering the entire small intestinal transit time (SITT) (Gazzaniga et al., 1994, 2008, 2009; Maroni et al., 2010). In addition, an enteric-soluble film is generally applied to such systems, in order to overcome unpredictable gastric emptying (Macchi et al., 2015; Sangalli et al., 2001). Time-dependent reservoir devices are widely coated with cellulosic ethers, such as hydroxypropyl methyl-cellulose (HPMC), hydroxypropyl cellulose (HPC), hydroxyethyl cellulose (HEC) and calcium or sodium carboxymethylcellulose (CMC), thanks to their behavior and also due to their consolidated safety, versatility and broad availability profiles (Li et al., 2005). When exposed to aqueous media, these polymers

undergo swelling, dissolution and/or erosion phenomena determining a delay in their complete removal. Therefore, when employed as coating barriers, the contact of the drug-containing core with biological fluids and, consequently, the release of drug are delayed. Lag time before drug release is basically programmed by selecting the appropriate swellable/erodible polymer as well as its viscosity grade, and the thickness of the coating applied or the plug used to close a capsule system. In the case of barriers based on HPMC, different viscosity grades and several coating techniques for the manufacturing of reservoir systems have been studied (Maroni et al., 2010). More recently, HPC was also processed by injection molding (IM) for the manufacturing of capsular containers (ChronoCap™) able to convey different drug preparations and release them after a predetermined lag phase (Gazzaniga et al., 2009, 2011b). IM is a hot-processing technique, well-established in the plastic industry, aimed at turning thermoplastic materials into solid objects with defined characteristics of shape and dimensions (Osswald et al., 2008; Zema et al., 2012). The feasibility of this technique to prepare capsular containers having specific drug release performances according to the pharmaceutical grade polymer employed has been recently demonstrated (Gazzaniga et al., 2011a; Zema et al., 2012, 2013a). HPC capsules (Chronocap™) were shown to yield a lag phase, both *in vitro* and *in vivo* and, when used as the substrate for enteric coating, met the compendial gastroresistance requirements while maintaining the subsequent pulsatile release performance (Macchi et al., 2015, 2016). Hence, they proved to be suitable for time-dependent colon delivery.

Based on these premises, the aim of the present work was to prepare by micromolding novel capsular devices for colonic drug delivery, combining the time-dependent approach with the microbiological strategy. Being composed of swellable/erodible polymers, able to provide a lag phase covering the SITT irrespective of the physiological variables, and polysaccharides sensitive to bacterial degradation, the capsular device should reach the

colon before rupture and promptly release its contents through *in situ* degradation of the partially hydrated/dissolved shell barrier.

MATERIALS AND METHODS

Materials

High-amylose maize starch, (Amylo® N-400, Roquette Pharma, FR) (Amylo) and hydroxypropyl modified starch, (Lycoat RS780, Roquette Pharma, FR) (Lycoat) were kindly provided by Roquette; hydroxypropyl methylcellulose, HPMC, (AffiniSol™ 15LV and 4M grades; Dow, US-CA) (HPMC15LV and HPMC4M, respectively) were kindly provided by Dow; polyethylene glycol, (PEG1500, Clariant Masterbatches, IT) (PEG1500); glycerol, (Pharmagel, IT); blue dye-containing preparation (Kollicoat® IR Brilliant Blue, BASF, DE); acetaminophen (Rhodia, IT).

Methods

Preparation of materials

All the polymers used were kept in an oven at 40°C for 24 h prior to use. Individual polymers were placed in a mortar and plasticizers were manually added under continuous mixing with the aid of a pestle; the amount of plasticizer is expressed as percentage by weight on the dry polymer. When blends of polymers were prepared, mixing step of the separately plasticized components was accomplished in a mortar by geometric dilutions.

Hot-melt extrusion

Hot-melt extrusion (HME) was performed with a counter-rotating twin-screw mini extruder (HAAKE™ MiniLab II, Thermo Scientific™, Illinois, US) equipped with two

conical screws (diameter 5/14 mm, length 109.5 mm). Plasticized materials were manually loaded into the extruder and pulled out from the die having dimension of 1x4 mm.

Injection molding

IM process was accomplished with a bench-top micromolding machine (BabyPlast 6/10P; Cronoplast S.L., Barcelona, Spain; Rambaldi S.r.l., Molteno, Lecco, IT) equipped with two different molds: *i*) a disk-shaped mold (\varnothing 30 mm) provided with a central gate and allowing to control the cavity thickness (200 and 600 μm of nominal thicknesses) and *ii*) a capsular mold furnished with a hot-runner and with two interchangeable inserts for the manufacturing of matching cap and body items of 600 μm nominal thickness.

Single plasticized polymers or polymeric blends were manually loaded in the plasticating unit of the IM machine and successively pushed in the injection chamber by means of the loading plunger. Afterwards, two different and consecutives injection pressures (P_1 - P_2), maintained for a selected time (t_1 - t_2), were applied by a piston moving according to two distinct chosen rates (v_1 - v_2), in order to inject the polymeric melt into the mold cavity. Since many formulations are taken into account, in the case of the manufacturing of disks, each of them was analyzed systematically for the setting of parameters. Firstly, the injection molding temperatures were set as during the HME process and then adjusted. Whereas, for injection pressures and injection rates, minimum values were set up and progressively increased until the obtaining of complete disks. Only in the case of Amylo-based disks, the molded items were also prepared loading in the IM machine pellets manually cut from extrudates (HAAKE™ MiniLab II, 105°C, screw rotational speed of 75 rpm; recorded torque values of 60 Ncm).

Process parameters for the manufacturing of disks and capsular devices are reported in the Results section, as a discussion topic.

Evaluation of the performance of extruded and molded items

The evaluation of the ability to withhold water and dissolve/erode of extrudates as well as molded disks was carried out. Extrudates and molded disks of 600 μm in thickness were immersed in 125 mL of phosphate buffer pH 6.8, 37 ± 0.5 °C, 120 rpm by magnetic stirring. Molded disks of both 200 and 600 μm in thicknesses were also evaluated when immersed in 100 mL of culture medium (CM) or culture medium inoculated with human fecal samples (CMB), 37 ± 0.5 °C, 80 rpm by horizontal shaking (Stuart SSM1 Mini Orbital Shaker, VWR, Pennsylvania, US) and under anaerobic conditions (5% CO_2 , 10% H_2 , 85% N_2). Culture medium was prepared by dissolving 5 g tryptone, 3 g yeast extract, 2.5 g NaCl, 1.5 g beef extract and 0.3 g l-cysteine hydrochloride hydrate in 1 L of distilled water (pH 7.0 ± 0.2) and subsequent sterilization in an autoclave (20 min at 115°C). Faeces of patients suffering from ulcerative colitis (UC) were diluted 1:200 with cysteinated Ringer solution; 2.5 mL of this suspension was diluted with culture medium to 100 mL. At pre-determined time points samples were withdrawn, manually dried from the excess of fluid and weighed (wet mass t_x). After this procedure, samples were dried in an oven at 60 °C until constant weight (dry mass t_x). Water uptake (WU) and residual dry mass (RDM) were calculated according to the following equations:

$$WU\% = [\text{wet mass } (t_x) - \text{dry mass } (t_x)] / \text{wet mass } (t_x) * 100 \quad (\text{eq. 1})$$

$$RDM\% = \text{dry mass } (t_x) / \text{dry mass } (t_0) * 100 \quad (\text{eq. 2})$$

Before testing, extrudates, manually cut into pieces having 25 mm length, and molded disks, die-cut into smaller ones ($\varnothing = 11$ mm), were accurately weighed to record the dry mass at t_0 . Samples ($n = 3$) were hung on an iron support specifically created; whereas in case of the blends Amylo:HPMC15LV and Amylo:HPMC4M ($n = 9$) disks were inserted in a 180 μm tubular mesh cut on purpose and closed at both ends with clips.

Molded disks were also tested for barrier performance by using them to close the donor compartment of manually-assembled cells modified from the extraction cells used in the dissolution test for transdermal patches (2.9.4. Dissolution test for transdermal patches - Cell method, Ph. Eur. 9.1) (Figure 1). The donor compartment was filled with about 20 mg of Kollicoat[®] IR Brilliant Blue as the coloured tracer. The test (n = 3) was performed by a dissolution apparatus USP II (Dissolution System 2100B, Distek, NJ-US) in 500 mL of acceptor medium, phosphate buffer solution pH 6.8, $37 \pm 0.5^\circ\text{C}$, 100 rpm paddle rotating speed. Barrier resistance was expressed as the lag phase before rupture of the disks highlighted by colouring of the acceptor medium.

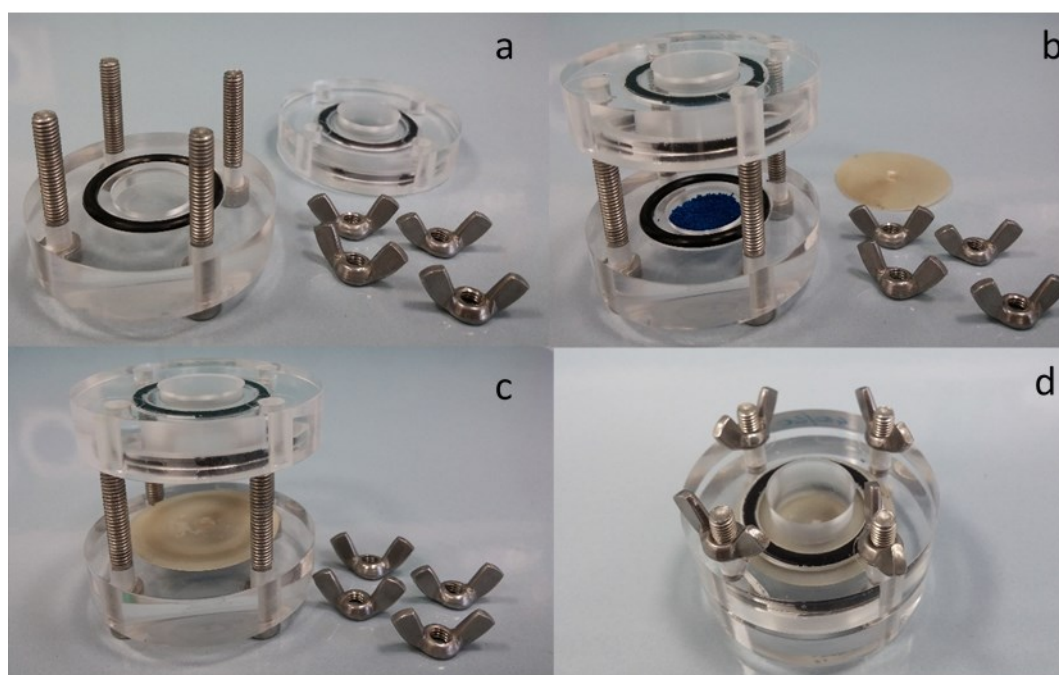


Figure 1. Cell for the evaluation of barrier performance of the molded polymeric disks: disassembled (a); partially assembled and filled with the tracer (b), equipped with the disk (c); finally assembled (d).

***In vitro* release performance from capsular devices**

Capsule bodies were manually filled with 50 mg of acetaminophen as a drug tracer and closed with matching caps. For the release test ($n = 3$), an adapted disintegration apparatus basket-rack assembly (BRA) was used to avoid sticking problems. The BRA moved at 31 cycles/min rate in separate vessels containing 800 mL of phosphate buffer pH 6.8, at 37 ± 0.5 °C. Fluid samples were automatically withdrawn at predetermined time points and spectrophotometrically (lambda25, Perkin Elmer, UK) assayed at $\lambda = 248$ nm. Times to the release of 10% and 90% of the conveyed drug ($t_{10\%}$ and $t_{90\%}$, respectively) and pulse time, which is the time elapsed between 10% and 90% release ($t_{10\%}$ and $t_{90\%}$), were calculated from the release curves.

RESULTS AND DISCUSSION

Evaluation of the hot-processability of materials



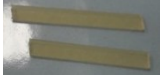

A wide range of pharmaceutical-grade polymers for both time-dependent and enzyme-triggered approach to colon delivery are available. High-amylose maize starch (*i.e.*, Amylo) and hydroxypropyl modified starch (*i.e.*, Lycoat) were selected as bacteria-sensitive polymers, based on some general findings relevant to their enzymatic biodegradability (Cummings et al., 1996b; Freire et al., 1996; Karrout et al., 2009a). Starch has been deeply investigated for decades for a variety of applications in the polymer, food and agriculture technology with results confirming its excellent feasibility for hot stage extrusion (Henrist & Remon, 1999). In addition, among the swellable/erodible polymers already known for the capability to generate reproducible lag phases prior to release when applied as coating barriers over drug-containing cores (Gazzaniga et al., 1994, 2006, 2011a; Sangalli et al., 2001, 2004), HPMC was preferred because a new modified grade

have been recently developed suitable for hot-processing (*i.e.*, AffiniSol™) (Huang et al., 2016). They maintain the crystallization inhibiting properties of traditional HPMC, but can be extruded over a wide temperature range in admixture with active ingredients, without the use of specific plasticizers (Dow Technical Bulletin).

Although these polymers have already been processed via hot-melt extrusion, their processability via injection molding still needs to be demonstrated.

A preliminary evaluation of the hot-processability of polymers was carried out by means of a twin screw extruder in order to identify the processing temperatures and select the type and the amount of plasticizers. Process conditions and formulation parameters relevant to extruded products with the best technological properties are reported in Table 1.

Table 1. Composition, aspect and process conditions of extruded products based on Amylo, Lycoat and AffiniSol™ polymers.

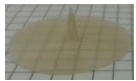
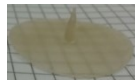
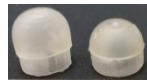
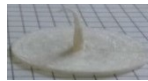
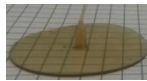

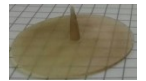

		Amylo-based extrudates	Lycoat-based extrudates	HPMC15LV-based extrudates	HPMC4M-based extrudates
Composition polymer and plasticizers (%w/w on polymer)		Amylo + 20% glycerol 15% water	Lycoat + 10% glycerol 5% water	AffiniSol™ HPMC15LV + 10% PEG1500	AffiniSol™ HPMC4M + 10% PEG1500
Process conditions	Temperature (°C)	105	100	145	170
	Screw rotational speed (rpm)	75	50	80	80
	Torque (Ncm)	60	80	40	60
Extruded product					

According to the literature, glycerol and water have been selected as the plasticizers for Amylo and Lycoat, that by applying heat and shear stresses are necessary to promote the formation of thermoplastic starch (TPS) (Forssell et al. 1997; Shogren et al. 1992). For the Amylo transition to TPS, higher amount of glycerol and water and higher screw rotational

speed were necessary, compared to Lycoat. In the case of HPMC, PEG1500 in the amount of 10% for both viscosity grades was enough to enable the achievement of extrudates with the desired properties (*e.g.*, dimensional stability, mechanical characteristics and surface aspects). From the visual analysis of all the extruded products, good homogeneity and transparency were noticed, indicating the actual polymer transition during the process.

Prior to the manufacturing of capsule shells, the first aim of IM studies was the achievement of circular screening items (*i.e.*, disks) by means of a specific mold. The simple shape of this mold, having a central injection point equidistant from all the extremities, was already shown useful for the evaluation of processability of different materials/composites (Macchi et al., 2015; Zema et al., 2013a, b). In addition, preliminary studies on the performance of materials intended for the preparation of release barriers (*i.e.*, coatings and capsules) could be undertaken exploiting the disk shape. Injection molding machines are generally fed with extruded pellets in order to overcome both mixing and flowing issues. In the case of starch, the HME step is pursued to allow the transition to TPS. However, the water content of the extrudates, when produced and after storage, could turn out critical for the IM process. Therefore, when working with Amylo, molded disks were prepared both from powders kneaded with the liquid plasticizing blend and from extruded pellets of the same initial composition. The obtained samples were compared on a quality level (*e.g.*, colour, transparency, rigidity) and for the behaviour after interaction with aqueous fluids, *i.e.*, on a performance level. The preparation of disks and capsular devices was carried out using the same composition of polymer-plasticizer established for HME process. The preliminary studies allowed the setup of the adequate process parameters (*i.e.*, temperature, injection pressure and time, as well as rate of the piston) for the manufacturing of disks, primarily, followed by the manufacturing of capsular containers; such results are reported in Table 2.

Table 2. IM process parameters used to obtain screening disks as well as capsular devices, and processability of the different materials.

		Amylo			Lycoat		HPMC15LV		HPMC4M	
		disk		capsule	disk	capsule	disk	capsule	disk	capsule
		<i>from powder</i>	<i>from extruded pellets</i>							
Temperatures (°C)	compression zone	110	110	110	110	115	155	165	175	175
	metering zone	115	120	115	125	125	165	170	180	180
	nozzle	130	140	130	135	135	175	180	190	190
	hot runner	/	/	135	/	140	/	190	/	200
Injection pressure P ₁₋₂ (bar)		70 - 60	70 - 60	70 - 60	70 - 60	80 - 70	50 - 30	30 - 10	60 - 50	30 - 10
Injection time t ₁₋₂ (s)		0.8 – 0.3	0.8 – 0.3	0.8 – 0.3	0.8 – 0.3	1.5 – 1.0	0.8 - 0.3	0.5 - 0.3	1.5 - 1.0	0.5 – 0.3
Piston rate v ₁₋₂ (%)		40 - 20	40 - 20	40 - 20	50 - 30	60 - 50	30 - 10	30 - 10	60 - 50	30 - 10
Processability*		-/+	-/+	-/+	-/+	-	+	-/+	+	-/+
Molded product						/				

*Processability: -, incomplete/broken/deformed item; -/+, not-automatically ejected/extremely adhesive item; +, automatically ejected item.

As shown in the Table 2, the processing temperatures of IM processes were slightly increased with respect to the HME ones. In particular, temperatures in the metering zone and in the nozzle needed to be higher in order to obtain an adequate fluidity of the melt when injected into the mold. Processability of materials has been evaluated on a quality level adapting an evaluation scale already used in a previous work (Melocchi et al., 2015). The scale ascribes a good processability to a material when molded objects are automatically ejected from the IM press, medium processability in case of not-automatically ejected items, particularly due to extremely adhesiveness and, finally, lacking processability when incomplete, broken or deformed items are obtained. Amylo was characterized by medium processability, independent of the method used to prepare the material, plasticized powder or prior-extruded pellets. Furthermore, as visible in the table, the process parameters used to prepare disks according to these two methods were the same, with the exception of temperatures which were slightly increased using pellets, probably due to the loss of water content occurred during HME process. Lycoat processability was very low because of recurring material blockage in the machine and rare attainment of complete and not deformed disks, whereas both viscosity grades of HPMC demonstrated good IM processability allowing the production of automatically ejected disks with satisfying technological properties.

Basing on results for the manufacturing of the disks, also capsular devices were prepared by the bench-top injection molding machine and relative process parameters were slightly modified from the ones referred to the manufacturing of disks for adapting them to the different design of the mold. For instance, temperatures were marginally increased, in particular in the hot runner, in order to keep a proper fluidity of the melt material and allow its progression into the cavity of the mold. Besides, also processability of materials turned out different, in particular, on average slightly worse than processability reported for the

disk-shape mold. Amylo and both HPMC had medium processability in order to manufacture capsular devices, in both cases, it was good enough to produce items having good properties such as reproducible weights and thicknesses and also proper shape of both bodies and caps for their matching. Whereas, in the case of capsular devices based on Lycoat, due to lacking of processability of this polymer, already described for the manufacturing of disks, capsules, hardly obtained, were characterized by incompleteness or impossibility to match bodies and caps without creating cracks of the shell; such features made them unsuitable for testing. Since capsular devices based on this modified starch do not represent the target product, and, in addition, they would not give interesting result due to Lycoat high solubility, no further efforts have been devoted to this formulation.

Evaluation of the performance of extruded and molded items

Water uptake and residual dry mass

WU and RDM profiles over 8 h relevant to extruded items and molded disks are shown in Figure 2. Tests were carried out in phosphate buffer pH 6.8 to mimic the small intestine environment. Extrudates and molded items were compared in order to assess the influence of the two hot-processing stages on the performance of the material.

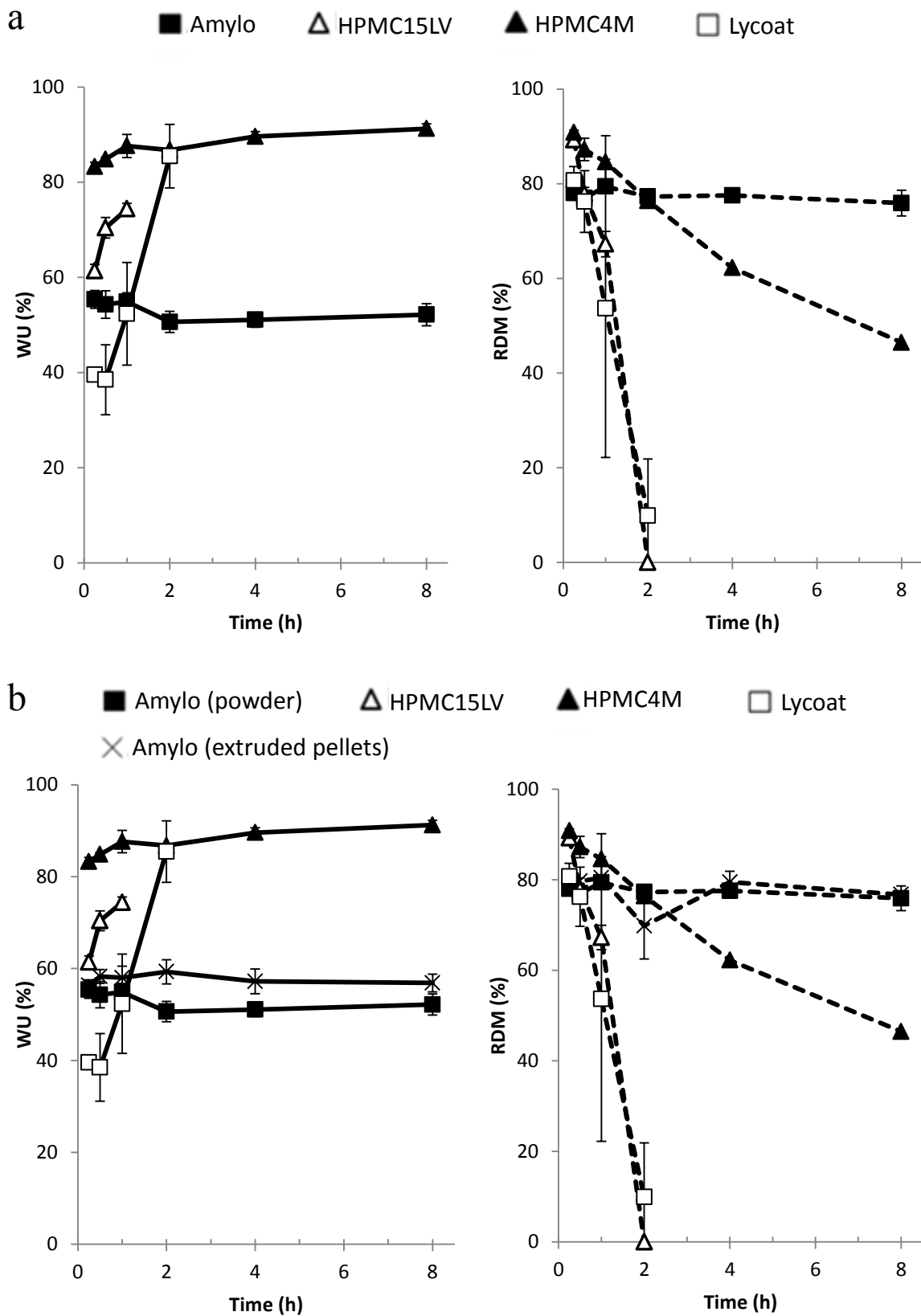


Figure 2. Water uptake and residual dry mass of (a) HME-extrudates based on Amylo, Lycoat, HPMC15LV and HPMC4M and (b) molded disks based on Amylo (molded from powder), Amylo (molded from extruded pellets), Lycoat, HPMC15LV and HPMC4M.

The total amount of water uptake upon exposure to phosphate buffer and the residual dry mass after the test were strictly dependent on the hydrophilicity and/or solubility of bacteria-sensitive polymers and on the viscosity grade of the swellable/erodible polymers. Amylo acquired moderate amount of water in a short time without any evident swelling neither changing in volume; furthermore, its residual dry mass was still very high after 8 hours. This may be explained by intrinsic resistance of this material due to the high amount of amylose. It is noteworthy that a great tendency of the material to exfoliation was noticed on the surface of the disks after few hours of test, as visible in Figure 3. Moreover, regarding the disks based on Amylo pre-extruded their appearance on a quality level was almost the same as disks based on the plasticized powder (Table 2), and, accordingly, their performance. Therefore, the extrusion step was demonstrated not compulsory to make starch thermoplastic.

Lycoat, which is a starch derivative modified to be easily soluble, is characterized by very fast water uptake and, consequently, mass loss, higher for HME samples which completely dissolved within 30 min. For IM samples, it took 2 h to completely dissolve and this can be ascribed to the higher density of the material promoted by the injection process.

In the case of HPMC, as expected, big amount of water was acquired due to its high hydrophilicity, greater for the higher viscosity grade with respect to the lower viscosity grade. For both viscosity grades, the mass of the items tended to decrease over time as a result of the swelling and consequent dissolution/erosion of hydrated portions. Samples based on the higher viscosity grade of HPMC were able to maintain about 45% or 75% of their mass after 8 hours, whereas those based on the lower viscosity grade eroded/dissolved within 4 hours or 2 hours, in both cases when extruded or molded, respectively. This can be explained by the formation of a gel structure upon exposure to PBS, very viscous, thick and resistant for the higher viscosity grade and thinner and less resistant for the lower one.



Figure 3. Amylo-based disks after 4 h interaction with aqueous fluids.

Barrier resistance of disks and in vitro release performance of capsular devices

IM disks were exploited for analyzing their resistance as polymeric barriers when used to close the donor compartment of modified permeability cells, and the lag time before their rupture was evaluated. In addition, drug release from capsular containers, initially carried out in PBS in order to investigate the performance of the devices, leaving aside the bacterial degradation effect, was evaluated. In detail, the time necessary for 10% of drug release, calculated from the release profiles, was used to define lag time of the capsular devices. In Table 3 lag times before rupture of disks are compared to lag times before 10% release of conveyed drug from capsular containers of analogous composition.

Table 3. Lag time before rupture of the disks and lag time before drug release from capsular devices.

	Lag time before rupture of the disks (h ± s.d.)	Lag time of capsular devices t_{10%} (h ± s.d.)
Amylo	0.47 ± 0.17	0.28 ± 0.05
Lycoat	0.62 ± 0.33	/
HPMC15LV	2.06 ± 0.64	1.36 ± 0.34
HPMC4M	> 8	4.14 ± 0.23

Amylo-based molded items showed a poor resistance in aqueous fluids. This behaviour was quite unexpected considering the good resistance to mass loss, previously described, of extruded and molded items based on Amylo. The fast rupture of Amylo disks and opening of capsular devices can be probably explained by the exfoliation behavior of the material (Figures 3 and 4). On the contrary, as expected, Lycoat confirmed its soluble nature acting as a barrier for a short time; the release performance of capsular containers was not assessed as they were not suitable for the test (generally incomplete, broken and/or deformed caps and bodies). In the case of the two HPMC grades, the lag times before the release for both disks and capsules are mutually coherent and in accordance with the results of RDM. The different lag phases between the two HPMC can be attributed once more to the characteristics of the swollen system. The slower erosion/dissolution of the gel barrier based on HPMC4M was also reflected in the opening behavior of capsules defined as pulse time, which is the time elapsed between 10% and 90% release, it turned out 1.57 ± 0.24 h for HPMC4M capsules as compared to 0.45 ± 0.24 h for HPMC15LV.

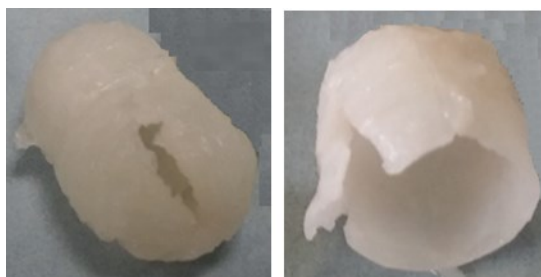






Figure 4. Breakage of capsular devices based on Amylo during dissolution test.

Polymeric blends for the manufacturing of combined systems

Taking into account the achievement of combined systems and the results obtained with single swellable/erodible and bacteria-sensitive polymers, Amylo and HPMC were selected as the most promising blend components. Therefore, preliminary studies on 1:1 blends of the microbiota-sensitive polymer with both the HPMC grades were undertaken. The use of Lycoat in the formulation of blends was confirmed very critical, especially when in admixture with the higher density grade of HPMC. Moreover, the promptly solubility shown by the molded disks prepared with it seems not promising in view of achieving capsular devices able to withstand the transit in the small intestine, *i.e.*, for almost 4 h. The possibility to check the behaviour of systems based on blends containing Lycoat will depend on the development of dedicated molds, which it is too challenging for the moment.

Processability studies on the blends were focused on the selection of temperature ranges allowing the glass transition of both the polymeric components. Interestingly, the best results were obtained when blends were prepared using the same type and amount of plasticizers needed by the single components. The process conditions used for the manufacturing of disks and capsular devices are reported in Table 4.

Table 4. IM process parameters used to obtain screening disks as well as capsular devices, and processability of the Amylo/HPMC blends.

		Amylo:HPMC15LV		Amylo:HPMC4M	
		disk	capsule	disk	capsule
Temperature (°C)	compression zone	125	125	135	135
	metering zone	125	125	135	135
	nozzle	135	135	155	155
	hot runner	/	145	/	160
Injection pressure P ₁₋₂ (bar)		50 – 30	30 – 20	60 – 50	70 – 60
Injection time t ₁₋₂ (s)		0.8 – 0.3	0.8 – 0.3	0.8 – 0.3	0.8 – 0.3
Piston rate v ₁₋₂ (%)		30 – 10	30 – 10	60 – 50	60 – 40
Processability*		-/+	-/+	-/+	-/+
Molded product					

*Processability: –, incomplete/broken/deformed item; -/+, not-automatically ejected/extremely adhesive item; +, automatically ejected item.

In order to obtain disks based on blends of HPMC with the bacteria-sensitive polymer, firstly, the process parameters have been selected in the middle way between the ones used for individual polymer and subsequently adjusted to the process, the same criterion was used for the manufacturing of capsular containers. In particular, processing temperatures were lowered with respect to temperatures used for processing HPMC alone, in order to limit the evaporation of water which represents an essential plasticizer of Amylo. Even if for the mixture of Amylo and HPMC manual ejection of molded products was required and lower processability, compared to individual HPMC, was noticed, product manufacturing was accomplished. Both disks and capsular devices were obtained with satisfying qualities; disks were characterized for water uptake, residual dry mass, and barrier resistance and *in vitro* drug release from capsular containers was assessed (Figures 5 and 6). For comparison

purposes data relevant to systems made of the single blend components, partially shown in Figure 2 and Table 3, are also reported.

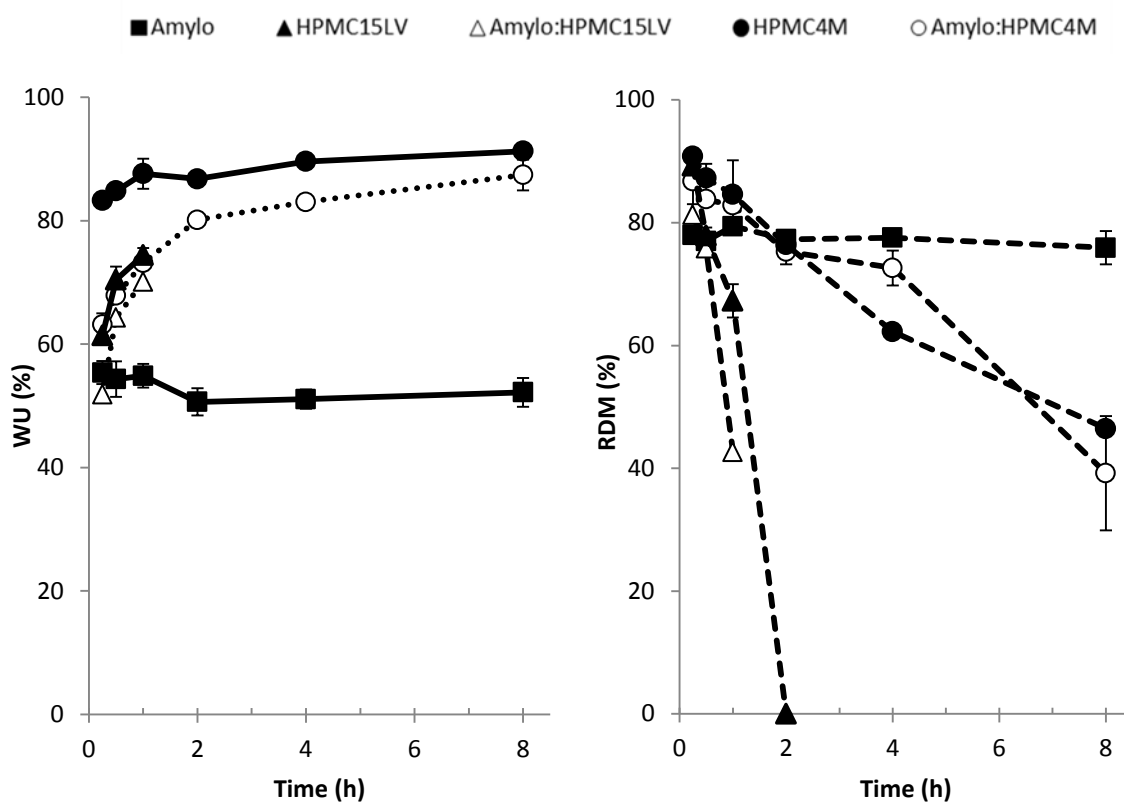


Figure 5. Water uptake and residual dry mass of molded disks based on Amylo, HPMC15LV and HPMC4M and respective blends 1:1 ratio Amylo:HPMC15LV and Amylo:HPMC4M.

Despite the 1:1 ratio of polymers, the behavior of the swellable/erodible polymer prevails on the behavior of the bacteria-sensitive component. The trends of WU% and RDM% of the blends are placed just below the trends of individual HPMCs, meaning that their behavior is intermediate between bacteria-sensitive polymer and swellable/erodible ones, with prevalence of the latter component.

The time before rupture of the disks follows the same trend: $2.21 \text{ h} \pm 0.25$ for Amylo:HPMC15LV and more than 8 h for blends of Amylo with HPMC4M. Capsular devices based on the polymeric blend with HPMC15LV showed a slight early opening,

with a reduce pulse time of about 4 min and a higher reproducibility of the release behavior compared to HPMC15LV-based capsules. Since no specific *in vitro-in vivo* correlation studies are available, the $t_{10\%}$ obtained *in vitro*, *i.e.*, 1.34 ± 0.00 h, was considered compatible with colon targeting, based on the results already obtained with the Chronocap™ System (Gazzaniga et al., 2011c). Considering the release profiles of devices based on the blend with HPMC4M, the lag time was increased with respect to that obtained with capsules based on the individual swellable/erodible polymer. This result seems to point out the ability of Amylo to slow down the hydration and dissolution/erosion of the swellable/erodible component, probably due to a competition towards water uptake. The quite long drug diffusion phase occurring across the shell of these devices and responsible for the very high pulse time, *i.e.*, 1.98 ± 0.20 h, could be limited in the presence of bacteria thanks to the degradation of the Amylo component of the capsule shell that would promote the loss of integrity of the wall barrier.

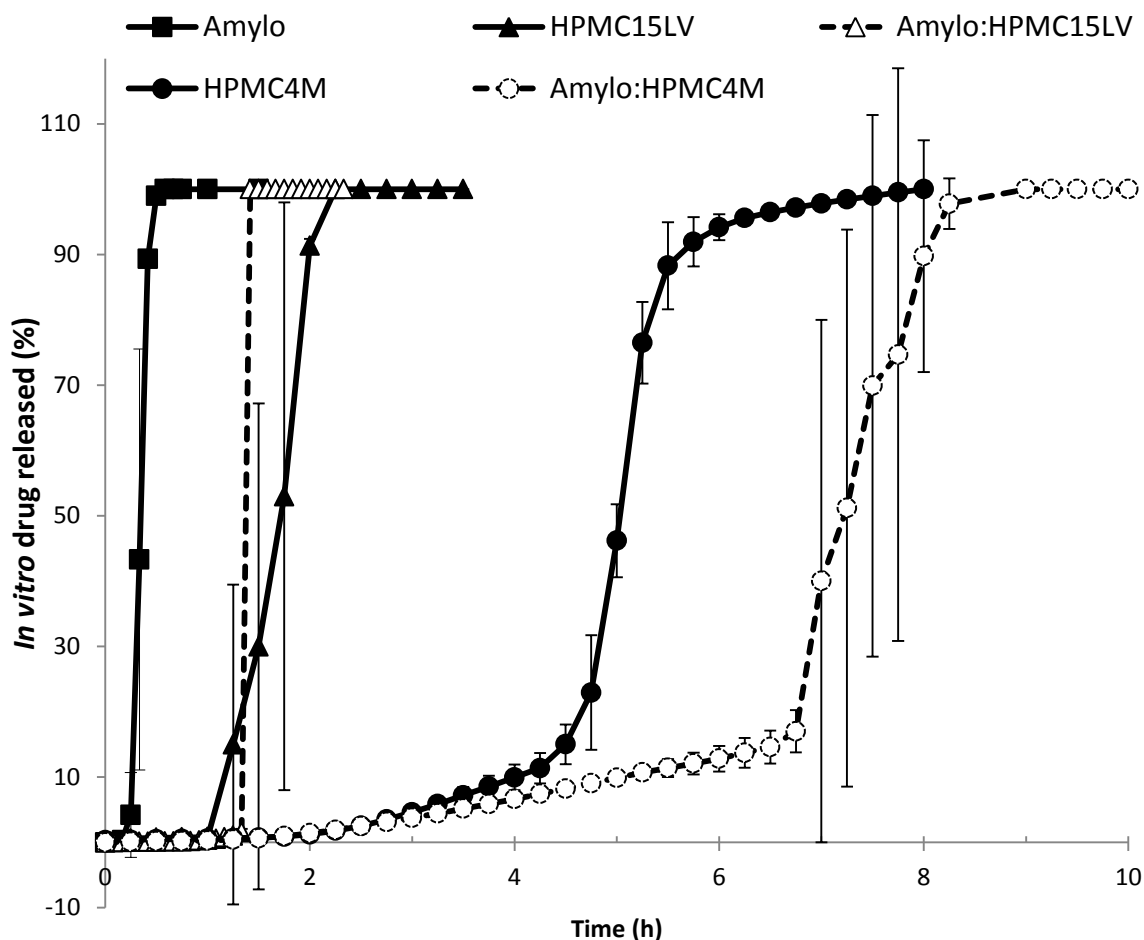


Figure 6. *In vitro* drug release of capsular devices based on Amylo, HPMC15LV and HPMC4M and their 1:1 blends.

Evaluation of the reliability of enzyme-triggered approach

In order to prove the actual sensitivity of the selected polymers to the colonic bacteria degradation, tests with microflora of patients suffering from ulcerative colitis were carried out. Molded Amylo-based barriers showed a good ability to acquire water that should be a promising feature for enzymes penetration into the material to promote degradation. WU and RDM of Amylo disks were determined upon exposure to fecal samples from UC patients. Since the test for bacteriological analysis has been developed for testing films (Karrout et al., 2009a), which are much thinner compared to the 600 μm thick disks and

capsule shells, in this step, also disks based on individual Amylo and the blend Amylo:HPMC4M of 200 μm in thickness were evaluated. These thinner disks were prepared according to process parameters reported in Table 5.

Table 5. Process parameters for manufacturing of molded disks of 200 μm thickness.

		Amylo	Amylo:HPMC4M
Temperatures (°C)	compression zone	110	135
	metering zone	115	135
	nozzle	130	155
Injection pressure P_{1-2} (bar)		80 – 70	90 – 80
Injection time t_{1-2} (s)		1.5 – 1.0	2.0 – 1.5
Piston rate v_{1-2} (%)		70 – 50	80 – 60

In Figure 7 results of water uptake and residual dry mass upon exposure to culture medium (CM) and culture medium inoculated with fecal samples (CMB) for 24 h and 48 h are reported.

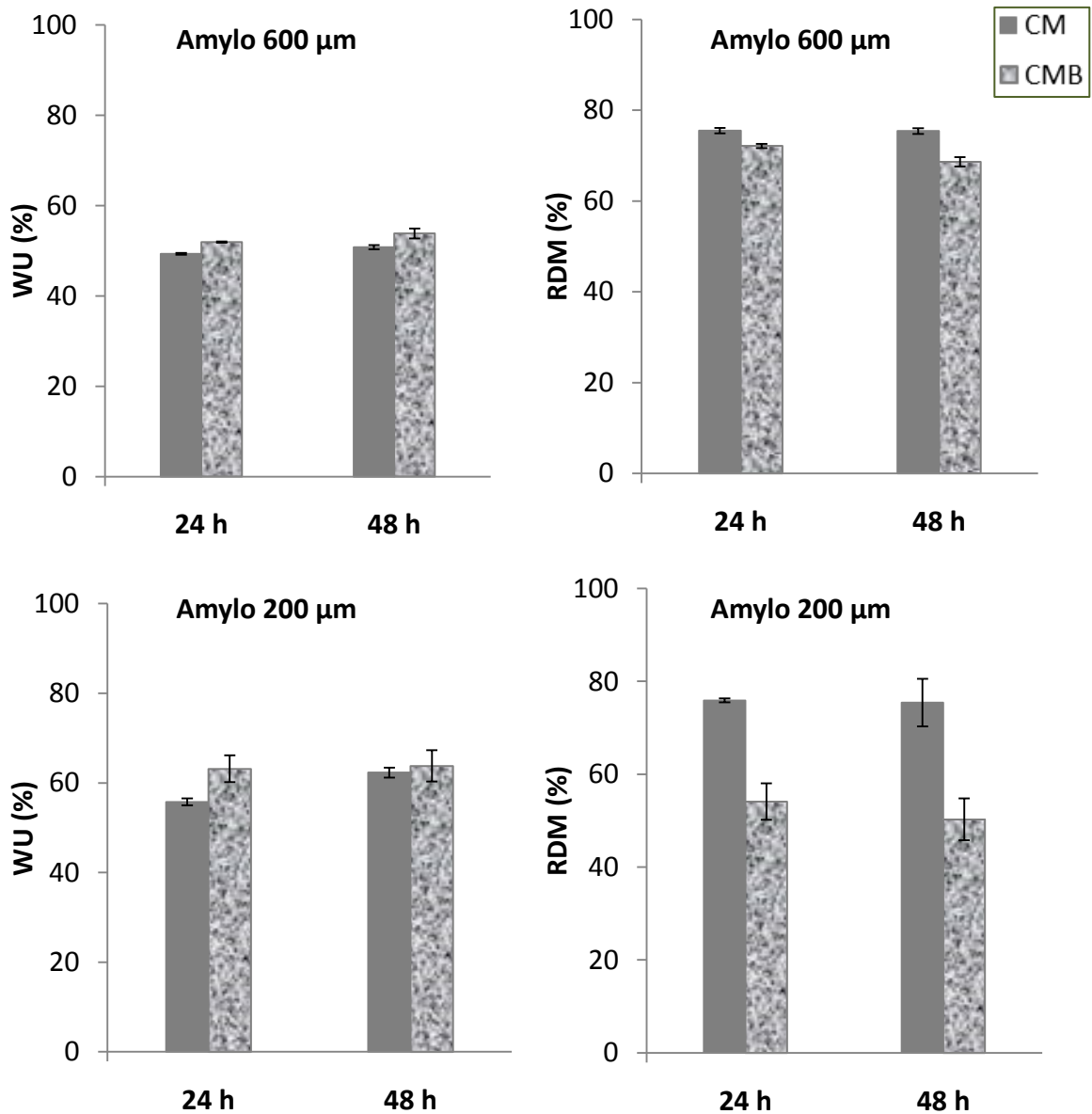


Figure 7. Water uptake and residual dry mass of Amylo disks (200 and 600 μm) upon exposure to CM or CMB for 24 and 48 h.

Molded disks of both thicknesses confirmed to acquire pronounced amounts of water and to maintain them over 2 days. WU values are somewhat higher for the 200 μm disks, probably thanks to the lower width to be penetrated; however, for each type of disk, *i.e.*, 200 and 600 μm thick, they are not significantly different over time and they are independent from the medium, CM or CMB. The mass loss behaviour in CM turned out independent from disk thickness as well as exposure time, and the RDM was generally

high, around 80%. On the contrary, when disks were in contact with the medium inoculated with faeces, RDM values were reduced up to 50% for the 200 μm thick samples, confirming the actual degradation performed by enzymes. In particular, additional mass loss is noticed after 48 h of incubation, in contrast to what was seen for samples in CM. In case of 600 μm thick disks, the degradation rate was lower, probably because the hydrodynamic conditions used for the incubation of samples is not enough to put in evidence the performance (non-discriminatory conditions), *i.e.*, not enough to remove higher amounts of eroded material per time unit.

The test conditions employed for disks based on Amylo were not applicable to disks based on the Amylo:HPMC15LV and Amylo:HPMC4M blends, because of the presence of a pronounced poorly consistent gel layer after the long times required for bacteria incubation. For this reason, disks were inserted in a tubular mesh, as described in method section, aimed at allowing the items to interact with the medium through all the surfaces and, simultaneously, preserving the sample integrity for recovering at the end of the test. Even though the presence of the mesh represents a limit of the test, the 180 μm dimension of this tool was chosen after several attempts as the best compromise for balancing the two phenomena just reported. As the blends already showed higher dissolution/erosion rate, the duration of the test was adjusted to shorter sampling time (15 h, 20 h, 40 h) and 48 h sampling time was discarded because characterized by very low residual masses challenging for being weighed.

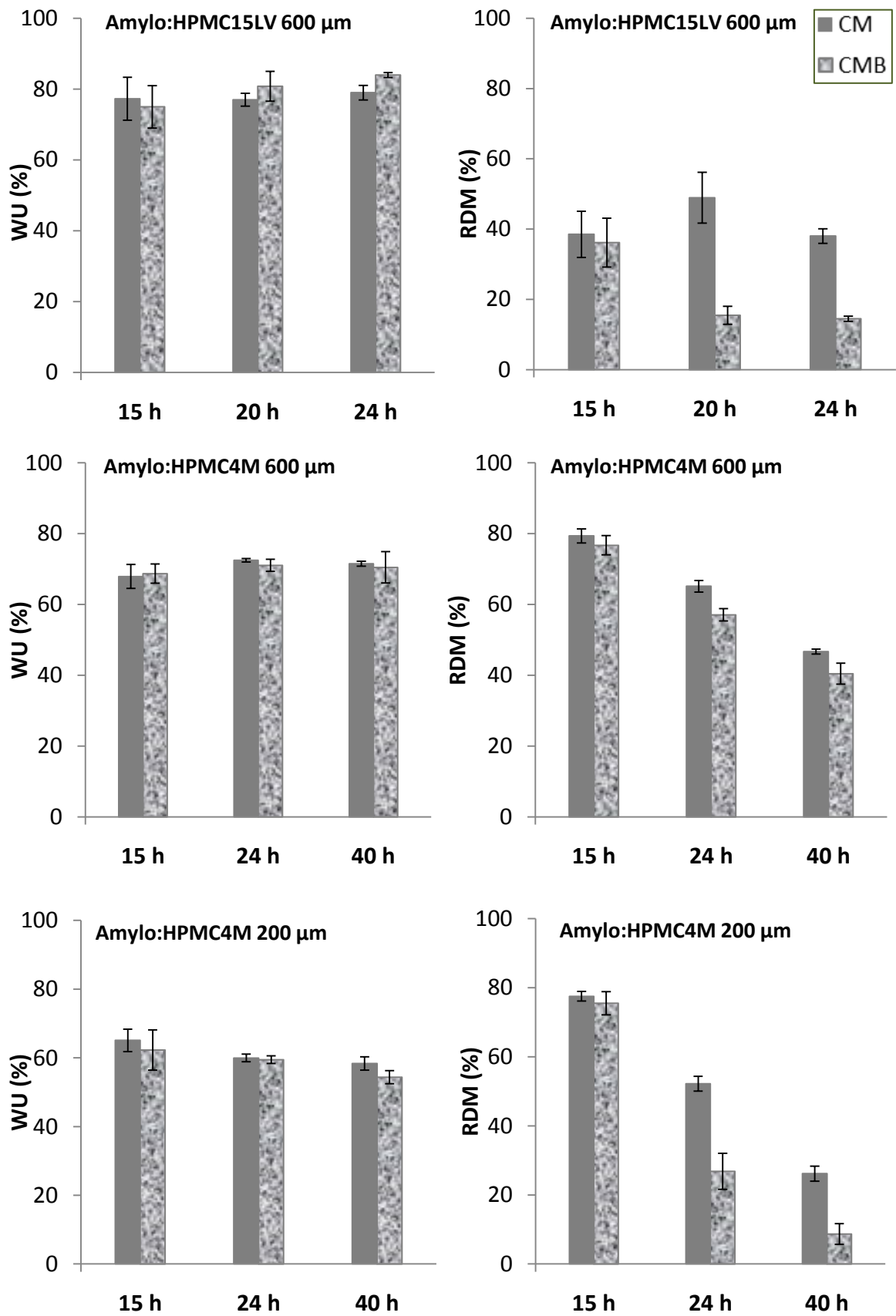


Figure 8. Water uptake and residual dry mass of disks based on Amylo:HPMC15LV (600 μm) and on Amylo:HPMC4M (600 and 200 μm) upon exposure to CM or CMB for 15, 20, 24 and 40 h.

As expected by the presence of an hydrophilic swellable/erodible polymer, WU of disks based on polymeric blends was higher with respect to Amylo disks (Figure 8). The ability to retain water is very similar comparing the two viscosity grades, slightly higher for the blend containing HPMC15LV, as well as comparing the different thicknesses. Besides, no significant differences in WU% values was noticed between CM and CMB, as occurred also for Amylo disks. For all the disks considered, upon exposure to CM, a mass loss progression is visible over time because HPMC undergoes swelling and consequent dissolution/erosion of gel portions, faster for the blend with HPMC15LV. Comparing 200 and 600 μm thickness disks based on Amylo:HPMC4M, no evident differences in mass loss were noticed, especially in shorter times, probably because of inappropriate hydrodynamic conditions for gel removal from the surface of the disks made worse by the use of the mesh which, anyway, is essential for samples withdrawal.

Mass loss of all the disks increased when the samples were dipped in CMB proving that the presence of bacteria in the medium allows the fermentation of the starch component. Even though the amount of the bacteria-sensitive polymer is equivalent in all the disks, the degree of degradation after incubation with fecal slurries is different considering the two viscosity grades. The reason of these results may lie in the different behavior of the two HPMC components after interaction with the medium. The less viscous gel of HPMC15LV dissolves and erodes, faster than HPMC4M, clearly, contributing to mass loss of the item and, at the same time, increasing the surface area of Amylo component exposed to the enzymes present in the medium; in fact, after 24 h of incubation with bacteria, the RDM% of disks based on Amylo:HPMC15LV is halved compared to the same value of disks obtained with the blend Amylo:HPMC4M. When two different thickness of disks based on Amylo:HPMC4M are compared, once again, mass loss evolve more quickly for the thinner disks.

By dint of these results, it was possible to confirm the actual sensitivity of molded Amylo, alone and in admixture with HPMC, towards bacterial degradation, as well as to understand that the different viscosity grades of the HPMC component could change the potential *in situ* performance of the molded barriers manufactured from Amylo/HPMC blends. In fact, with high viscous gel, since the dissolution/erosion of such layer is slow, Amylo can be hidden and its accessibility by enzymes reduced, with the consequence of lengthier Amylo degradation. Such possibility of modulating the degradation performance represents an advantageous aspect for the development of a platform for colon delivery. Moreover, in order to fine-tune the performance of the capsular platform, also attempts at changing the HPMC and Amylo ratio could be carried out.

CONCLUSIONS

In the present work, the feasibility of combining time-dependent and microbiological approaches to target colonic release, while overcoming specific limitations of each strategy, was proved. Polymeric barriers in the form of molded capsular devices were successfully prepared based on *i*) swellable/erodible materials, selected to provide a lag phase covering the small intestine transit of the system (time-dependent approach), and *ii*) bacteria-sensitive polymers, chosen to ensure that the lag phase would not largely exceed the small intestinal transit and to improve the prompt release of capsule contents through *in situ* degradation (enzyme-triggered approach).

A colon delivery platform consisting of capsular devices prepared by IM based on blends of HPMC and high-amylose maize starch was in particular developed. The hot-processability of selected materials, when considered alone and in admixture with each

other, was demonstrated through preliminary studies aimed at the identification of process parameters and type/amount of plasticizers. Moreover, the sensitivity to colonic bacteria degradation of the high-amylose starch processed by IM, both alone and in admixture with different HPMC grades, was assessed. Since great care has to be taken when defining experimental conditions for drug release measurements from systems intended for colon delivery, and even more for systems containing swellable/erodible component, next studies should focus on the research of the condition for the *in vitro* drug release able to discriminate differences not yet discernible.

REFERENCES

- Amidon, S., Brown, J.E., & Dave, V.S. (2015). Colon-Targeted Oral Drug Delivery Systems: Design Trends and Approaches. *AAPS PharmSciTech*, 16, 731–741.
- Bourgeois, S., Harvey, R., & Fattal, E. (2005). Polymer colon drug delivery systems and their application to peptides, proteins, and nucleic acids. *American Journal of Drug Delivery*, 3, 171–204.
- Cerchiara, T., Abruzzo, A., Parolin, C., Vitali, B., Bigucci, F., Gallucci, M.C., Nicoletta, F.P. & Luppi, B. (2016). Microparticles based on chitosan/carboxymethylcellulose polyelectrolyte complexes for colon delivery of vancomycin. *Carbohydrate Polymers*, 143, 124–130.
- Cummings, J.H., Beatty, E.R., Kingman, S.M., Bingham, S.A., & Englyst, H.N. (1996a). Digestion and physiological properties of resistant starch in the human large bowel. *The British Journal of Nutrition*, 75, 733–747.
- Cummings, J.H., Milojevic, S., Harding, M., Coward, W.A., Gibson, G.R., Louise Botham, R., Ring, S.G., Wraight, E.P., Stockham, M.A., Allwood, M.C., & Newton, J.M. (1996b). In vivo studies of amylose- and ethylcellulose-coated [¹³C]glucose microspheres as a model for drug delivery to the colon. *Journal of Controlled Release*, 40, 123–131.
- Davis, S.S. (1985). The design of evaluation of controlled release systems for the gastrointestinal tract. *Journal of Controlled Release*, 2, 27–38.
- Davis, S.S., Hardy, J.G., & Fara, J.W. (1986). Transit of pharmaceutical dosage forms through the small intestine. *Gut*, 27, 886–892.
- Dow Pharma & Food Solutions – Technical Bulletin:
http://msdssearch.dow.com/PublishedLiteratureDOWCOM/dh_0954/0901b803809543f4.pdf?filepath=dowwolff/pdfs/noreg/198-02327.pdf&fromPage=GetDoc
- Englyst, H.N., Kingman, S.M., Hudson, G.J., & Cummings, J.H. (1996). Measurement of resistant starch in vitro and in vivo. *British Journal of Nutrition*, 75, 749–755.
- Forssell, P. M., Mikkilä, J. M., Moates, G. K., & Parker, R. (1997). Phase and glass transition behaviour of concentrated barley starch-glycerol-water mixtures, a model for thermoplastic starch. *Carbohydrate Polymers*, 34, 275–282.

- Freire, C., Podczec, F., Veiga, F., & Sousa, J. (2009). Starch-based coatings for colon-specific delivery. Part II: Physicochemical properties and in vitro drug release from high amylose maize starch films. *European Journal of Pharmaceutics and Biopharmaceutics*, 72, 587–594.
- Gazzaniga, A., Cerea, M., Cozzi, A., Foppoli, A., Maroni, A., & Zema, L. (2011a). A novel injection-molded capsular device for oral pulsatile delivery based on swellable/erodible polymers. *AAPS PharmSciTech*, 12, 295–303.
- Gazzaniga, A., Cerea, M., Cozzi, A., Foppoli, A., Sangalli, M.E., Tavella, G., & Zema, L. (2011b). Pharmaceutical dosage forms for time-specific drug delivery. Patent US 2011/0229530 A1.
- Gazzaniga, A., Cerea, M., Cozzi, A., Foppoli, A., Zema, L., Maroni, A., & Sangalli, M.E., (2009). Injection-molded swellable/erodible capsular devices intended for oral pulsatile delivery. *Transactions of the Annual Meeting of Controlled Release Society* 36, 335.
- Gazzaniga, A., Foppoli, A., Maroni, A., Cozzi, A., Macchi, E., & Cerea, M. (2011c). Injection-molded capsular device for oral pulsatile delivery: an in vivo evaluation. In: *38th CRS Annual Meeting & Exposition of the Controlled Release Society 2011 - July 30–August 3, National Harbor, Maryland.*
- Gazzaniga A., Maroni A., Foppoli A., & Palugan L., (2009), Oral colon delivery: rationale and time-based drug design strategy, *Discovery Medicine*, 6, 223-228.
- Gazzaniga, A., Maroni, A., Sangalli, M.E., & Zema, L. (2006). Time-controlled oral delivery systems for colon targeting. *Expert Opinion on Drug Delivery*, 3, 583–597.
- Gazzaniga, A., Palugan, L., Foppoli, A., & Sangalli, M. E. (2008). Oral pulsatile delivery systems based on swellable hydrophilic polymers. *European Journal of Pharmaceutics and Biopharmaceutics*, 68, 11–18.
- Gazzaniga, A., Sangalli, M.E., & Giordano, F. (1994). Oral Chronotopic® drug delivery systems: achievement of time and/or site specificity. *European Journal of Pharmaceutics and Biopharmaceutics*, 40, 246–250.
- Harding, D.R.K. (2016). Design and evaluation of a novel chitosan-based system for colon-specific drug delivery. *International Journal of Biological Macromolecules*, 85, 539-546.

- Henrist, D., & Remon, J.P. (1999). Influence of the formulation composition on the in vitro characteristics of hot stage extrudates. *International Journal of Pharmaceutics*, *188*, 111-119.
- Huang, S., O'Donnell, K. P., Keen, J. M., Rickard, M. A., McGinity, J. W., & Williams, R. O. (2016). A New Extrudable Form of Hypromellose: AFFINISOL™ HPMC HME. *AAPS PharmSciTech*, *17*, 106–119.
- Karrout, Y., Dubuquoy, L., Piveteau, C., Siepmann, F., Moussa, E., Wils, D., Beghyn, T., Neut, C., Flament, M.-P., Guerin-Deremaux, L., Dubreuil, L., Deprez, B., Desreumaux, P., & Siepmann, J. (2015). In vivo efficacy of microbiota-sensitive coatings for colon targeting: A promising tool for IBD therapy. *Journal of Controlled Release*, *197*, 121–130.
- Karrout, Y., Neut, C., Wils, D., Siepmann, F., Deremaux, L., Dubreuil, L., Desreumaux, P., & Siepmann, J. (2009a). Colon targeting with bacteria-sensitive films adapted to the disease state. *European Journal of Pharmaceutics and Biopharmaceutics*, *73*, 74–81.
- Karrout, Y., Neut, C., Wils, D., Siepmann, F., Deremaux, L., Flament, M.-P., Dubreuil, L., Desreumaux, P., & Siepmann, J. (2009b). Novel polymeric film coatings for colon targeting: Drug release from coated pellets. *European Journal of Pharmaceutical Sciences*, *37*, 427–433.
- Li, C.L., Martini, L.G., Ford, J.L., & Roberts, M. (2005). The use of hypromellose in oral drug delivery. *The Journal of Pharmacy and Pharmacology*, *57*, 533–546.
- Liu, L., Fishman, M.L., Kost, J., & Hicks, K.B. (2003). Pectin-based systems for colon-specific drug delivery via oral route. *Biomaterials*, *24*, 3333–3343.
- Macchi, E., Zema, L., Maroni, A., Gazzaniga, A., & Felton, L.A. (2015). Enteric-coating of pulsatile-release HPC capsules prepared by injection molding. *European Journal of Pharmaceutical Sciences*, *70*, 1–11.
- Macchi, E., Zema, L., Pandey, P., Gazzaniga, A., & Felton, L. A. (2016). Influence of temperature and relative humidity conditions on the pan coating of hydroxypropyl cellulose molded capsules. *European Journal of Pharmaceutics and Biopharmaceutics*, *100*, 47–57.
- Macfarlane, G.T., & Englyst, H.N. (1986). Starch utilization by the human large intestinal microflora. *Journal of Applied Microbiology*, *60*, 195–201.

- Maroni, A., Del Curto, M.D., Zema, L., Foppoli, A., & Gazzaniga, A. (2013). Film coatings for oral colon delivery. *International Journal of Pharmaceutics*, 457, 372–94.
- Maroni, A., Zema, L., Del Curto, M.D., Loreti, G., & Gazzaniga, A. (2010). Oral pulsatile delivery: Rationale and chronopharmaceutical formulations. *International Journal of Pharmaceutics*, 398, 1–8.
- McConnell, E.L., Short, M.D., & Basit, A.W. (2008). An in vivo comparison of intestinal pH and bacteria as physiological trigger mechanisms for colonic targeting in man. *Journal of Controlled Release*, 130, 154–160.
- Melocchi, A., Loreti, G., Del Curto, M. D., Maroni, A., Gazzaniga, A., & Zema, L. (2015). Evaluation of hot melt extrusion and injection molding for continuous manufacturing of immediate release tablets. *Journal of Pharmaceutical Sciences*, 104, 1971–1980.
- Osswald, T.A., Turng, L.-S., & Gramann, T.J. (2008). Injection Molding Materials. In Hanser (Ed.), *Injection Molding Handbook* (2nd ed., pp. 19–61). Ohio.
- Patel, M.C., & Amin, A. (2011). Recent trends in microbially and/or enzymatically driven colon-specific drug delivery systems. *Critical ReviewsTM in Therapeutic Drug Carrier Systems*, 28, 489–552.
- Prasad, Y.V, Krishnaiah, Y.S., & Satyanarayana, S. (1998). In vitro evaluation of guar gum as a carrier for colon-specific drug delivery. *Journal of Controlled Release*, 51, 281–287.
- Ring, S.G., Gee, J.M., Whittam, M., Orford, P., & Johnson, I.T. (1988). Resistant starch: Its chemical form in foodstuffs and effect on digestibility in vitro. *Food Chemistry*, 28, 97–109.
- Sangalli, M. E., Maroni, A., Foppoli, A., Zema, L., Giordano, F., & Gazzaniga, A. (2004). Different HPMC viscosity grades as coating agents for an oral time and/or site-controlled delivery system: a study on process parameters and in vitro performances. *Journal of Pharmaceutical Sciences*, 22, 469–476.
- Sangalli, M.E., Maroni, A., Zema, L., Busetti, C., Giordano, F., & Gazzaniga, A. (2001). In vitro and in vivo evaluation of an oral system for time and/or site-specific drug delivery. *Journal of Controlled Release*, 73, 103–110.
- Seeli, D.S., & Prabakaran, M. (2016). Guar gum succinate as a carrier for colon-specific drug delivery. *International Journal of Biological Macromolecules*, 84, 10–15.

- Shogren, R. L., Swanson, C. L., & Thomson, A. R. (1992). Extrudates of Cornstarch with Urea and Glycols: Structure/Mechanical Property Relations. *Starch/Starke*, 44, 335–338.
- Sinha, V.R., Singh, A., Kumar, R.V, Singh, S., Kumria, R., & Bhinge, J.R. (2007). Oral Colon-Specific Drug Delivery of Protein and Peptide Drugs. *Critical ReviewsTM in Therapeutic Drug Carrier Systems*, 24, 63–92.
- Tung, N.T., Pham, T.M.H., Nguyen, T.H., Pham, T.T., & Nguyen, T.Q. (2016). Pectin/HPMC dry powder coating formulations for colon specific targeting tablets of metronidazole. *Journal of Drug Delivery Science and Technology*, 33, 19–27.
- Van den Mooter, G. (2006). Colon drug delivery. *Expert Opinion on Drug Delivery*, 3, 111–25.
- Wong, T.W., Colombo, G., & Sonvico, F. (2011). Pectin matrix as oral drug delivery vehicle for colon cancer treatment. *AAPS PharmSciTech*, 12, 201–214.
- Zema, L., Loreti, G., Macchi, E., Foppoli, A., Maroni, A., & Gazzaniga, A. (2013a). Injection-molded capsular device for oral pulsatile release: development of a novel mold. *Journal of Pharmaceutical Sciences*, 102, 489–499.
- Zema, L., Loreti, G., Melocchi, A., Maroni, A., & Gazzaniga, A. (2012). Injection Molding and its application to drug delivery. *Journal of Controlled Release*, 159, 324–331.
- Zema, L., Loreti, G., Melocchi, A., Maroni, A., Palugan, L., & Gazzaniga, A. (2013b). Gastroresistant capsular device prepared by injection molding. *International Journal of Pharmaceutics*, 440, 264–272.

Conclusions

Hot-processing and transformation of polymeric materials represent a very promising tool in several production areas, including the pharmaceutical one, where they are especially applied to the development of new drug delivery systems. In addition, the use of innovative manufacturing techniques, generally derived from other industrial fields, with the purpose of reducing time as well as costs of production, and allowing the patentability of the obtained drug products is pursued. In this respect, injection molding (IM) and micromolding (μ IM), widely employed within the plastic industry for a fast production of objects with whatever size and shape, have recently found application in the development of dosage forms. Therefore, interests about the research and the selection of pharmaceutical-grade polymeric materials suitable for withstanding hot-processes is also growing.

Starting from the experience concerning the manufacturing of reservoir systems gained by the Laboratory Team where I've carried out my PhD, the research activity was focused on the development of micromolded delivery platforms in the form of capsular containers for modified release of the conveyed drug, in particular, for both prolonged and site-specific release into the colon. Many of the outcomes achieved during the research activity, were possible thanks to collaborations, which have been established with other groups having different expertise, leading to a multidisciplinary approach of the research. All these co-operations have proved to be very fruitful especially for the different contributions

given for pursuing the predetermined goals. Moreover, thanks to the support of different experts, I had the possibility to broaden my knowledge to the rheological, material engineering and microbiological fields.

As regards the first (Chapter I and II) and the second part (Chapter III) of the PhD research activity, the hot-processability of a variety of materials was demonstrated and the feasibility of the micromolding process in the manufacturing of capsular containers was proved. In addition, the results obtained allowed to deepen the scientific knowledge relevant to the rheological and thermal characteristics of these pharmaceutical polymers, that would represent a useful tool for new applications in the field. Enriched and innovative information about their technological characteristics and performance when hot-processed were also collected, that represent the starting point for the further development of the systems proposed. The research, in fact, is still ongoing with new objectives. Also the identification of new methods purposely-developed for the evaluation of hot-processed systems need to be enhanced. Finally, a decisive stimulus for the research would derived from *in vivo* studies.